

Properties of Steady States for Thin Film Equations

R. S. LAUGESEN¹ and M. C. PUGH²

¹ *Department of Mathematics, University of Illinois, Urbana, IL 61801 USA*

² *Department of Mathematics, University of Pennsylvania, Philadelphia, PA 19104 USA*

(Received in revised form 20 January 1999)

We consider nonnegative steady-state solutions of the evolution equation

$$h_t = -(f(h)h_{xxx})_x - (g(h)h_x)_x.$$

Our class of coefficients f, g allows degeneracies at $h = 0$, such as $f(0) = 0$, as well as divergences like $g(0) = \pm\infty$.

We first construct steady states and study their regularity. For $f, g > 0$ we construct positive periodic steady states, and nonnegative steady states with either zero or nonzero contact angles. For $f > 0$ and $g < 0$, we prove there are no nonconstant positive periodic steady states or steady states with zero contact angle, but we do construct nonnegative steady states with nonzero contact angle.

In considering the volume, length (or period) and contact angle of the steady states, we find a rescaling identity that enables us to answer questions such as whether a steady state is uniquely determined by its volume and contact angle. Our tools include an improved monotonicity result for the period function of the nonlinear oscillator.

We also relate the steady states and their scaling properties to a recent blow-up conjecture of Bertozzi and Pugh.

1 Introduction

Equations of the type

$$h_t = -\nabla \cdot (f(h)\nabla\Delta h) - \nabla \cdot (g(h)\nabla h)$$

are used to model the dynamics of thin films of viscous fluids. The air/liquid interface is at height $z = h(x, y, t)$ and the liquid/solid interface is at $z = 0$. The coefficient $f(h)$ reflects surface tension effects — a typical choice is $f(h) = h^3 + \lambda h^n$ where $0 < n < 3$ and $\lambda \geq 0$ [21, 23, 27, 28, 33, 37]. The coefficient of the second-order term can reflect additional forces such as gravity $g(h) \sim h^3$ [22], van der Waals interactions $g(h) \sim h^m, m < 0$ [19, 30, 37, 48], or thermocapillary effects $g(h) \sim h^2/(1 \pm ch)^2$ [38, 47]. For a thin viscous film of liquid coating the inner wall of a straight pipe, the curvature gives rise to $g(h) \sim h^3$ [29, 31]. Also, such an equation is used to model a gravity-driven Hele–Shaw cell, with $f(h) \sim h$ and $g(h) \sim h$ [26, 25]. The aggregation of aphids on a leaf can similarly be modeled [32] with $f(h) \sim h$ and $g(h) \sim h - c$, where h represents the population density. In all of these cases h is a nonnegative function, representing a density, a film thickness, or a neck thickness.

We study the one-dimensional case, where $h = h(x, t)$ and the liquid film is uniform in the y direction:

$$h_t = -(f(h)h_{xxx})_x - (g(h)h_x)_x. \quad (1.1)$$

We consider steady states $h(x)$ that either are positive and periodic or are nonnegative with bounded support. Positive steady states correspond to a situation where the whole surface is wetted. Nonnegative steady states could be zero in entire regions or at isolated points, as in Figure 1, and could be made up of many separate droplets. For example, liquid hanging from the ceiling rarely collects itself into one large droplet — more often it evolves to a configuration of droplets, such as shown in Figure 1 (the ceiling is at the bottom). However, as we are studying the steady states, there is no harm in considering each steady droplet separately: we restrict h to a bounded interval (c, d) on which it is positive, with h equaling zero at c and d . We call this a “touchdown” steady state to emphasize the key difference between it and the positive periodic steady states. The

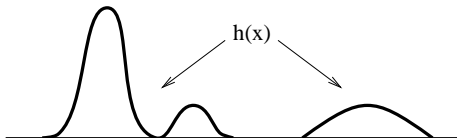


FIGURE 1.

“contact line” of a touchdown steady state is the boundary of its support, and the “contact angle” is determined by the slope h_x at the contact line. We consider only acute contact angles: h_x is finite.

We address four main issues in this paper:

- (i) steady states for the evolution equation with general coefficients f and g (Section 2);
- (ii) the construction and regularity of steady states, both touchdown and positive periodic, when f and g are power laws (Sections 3 and 4);
- (iii) relations between the length/period, volume and contact angle of steady states, in the power-law case (Section 5);
- (iv) connection to a finite-time blow-up conjecture of Bertozzi and Pugh [13] (Section 8).

As part of the third issue we ask: given an arbitrary choice of period and volume (per period), does there exist a positive periodic steady state with those values? Can two different steady states have the same period and volume? These questions are interesting because volume is preserved by the evolution equation.

We show one cannot always arbitrarily specify the volume and period. There are cases where there is no steady state with period P and volume V , unless P and V satisfy an inequality of the form

$$0 < V_1(P) \leq V \leq V_2(P) < \infty$$

for certain explicit upper and lower bounds V_1 and V_2 . For touchdown steady states we find analogous constraints on specifying the length and volume, or contact angle and length, or contact angle and volume. These are reminiscent of the length-determined

volume constraint found in Tuck and Schwartz's study [46] of a thin static droplet on a vertical surface, which is another situation with competition between a stabilizing surface tension and a destabilizing gravity force. (See §5.2.)

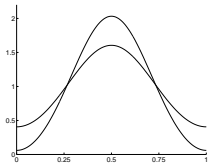


FIGURE 2.

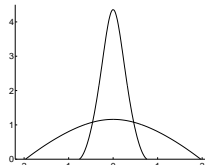


FIGURE 3.

Even if a steady state with the specified volume and length (or period) does exist, we find that it is not always unique: Figure 2 shows a pair of positive steady states with the same period and volume and Figure 3 shows a pair of touchdown steady states with the same volume and contact angle. These figures are discussed in §6.1 and §6.2, respectively.

Prior Work and Standing Assumptions

We now briefly discuss some background and prior work on evolution equations of the type (1.1), and explain our standing assumptions on the coefficients f, g , and the steady states h .

The signs of f and g affect the dynamics of solutions of (1.1). If we assume $f > 0$ then the equation is linearly well-posed about each constant steady state $h \equiv \bar{h} > 0$. If also $g(\bar{h}) \leq 0$ then small perturbations $\epsilon(t)\cos(kx)$ will decay for all modes k , but if $g(\bar{h}) > 0$, there will be a band ($0 < |k| < k_0$) of modes that grow. For this reason, we refer to the evolution equation with $f, g > 0$ as the “long-wave unstable equation”, and when $f > 0, g \leq 0$ we call it the “long-wave stable equation”.

If $f(y) < 0$ for some value of y then the evolution equation (1.1) is linearly ill-posed. Linear ill-posedness of an equation does not preclude the existence of solutions: there could be real-analytic solutions [17], or solutions with certain weak properties [3]. However existence results are currently known for (1.1) only for the linearly well-posed case $f \geq 0$.

Indeed, existence and regularity of nonnegative periodic weak solutions with zero contact angles has been proved for the $f \geq 0$ and $g \equiv 0$ case [5, 8, 12] as well as for the $f \geq 0$ and $g \not\equiv 0$ case [11, 13], for a range of degenerate coefficients, $f(0) = g(0) = 0$. Further, Bernis [6, 7] proved the contact lines have finite speed of propagation for the pure fourth-order equation; his methods extend naturally in the presence of a second-order term [13]. There has also been extensive work on the two-dimensional case where $h = h(x, y, t)$; we refer readers to a paper of Dal Passo, Garcke, and Grün for further references [41]. For the special case of $f(h) = h, g(h) \equiv 0$, Otto [40] used variational methods to prove the existence of solutions with nonzero contact angles. Also, Beretta [4] has proven the existence of compactly supported self-similar source-type solutions for the special case of $f(h) = h^n, g(h) = \pm h^{n+2}$, with $0 < n < 3$.

All of the above existence results are for degenerate coefficients; the existence theory does not include cases in which the coefficient $g(h)$ of the second-order term diverges as $h \downarrow 0$. Equations with divergent g have been proposed to model thin liquid films that rupture at isolated points, creating spots of dry exposed surface [15, 48], and to model

thin liquid films with precursor films [19, 30]. (For certain fluids on certain surfaces, van der Waals forces can be effective on a mesoscopic scale, creating a precursor film — a thin film that advances onto the dry surface ahead of the bulk of the fluid.) Bertozzi and Pugh [11] proposed a “porous-medium cut-off” of such divergent coefficients. They argued that since the divergence of $g(h)$ is a problem only as $h \downarrow 0$, this issue is mathematical rather than physical — the evolution equation (1.1) was derived using a continuum approximation, which is not intended to model the interface dynamics below certain length-scales.

However, we cannot exclude the possibility that an evolution equation with $f(h) \downarrow 0$ and a divergence $|g(h)| \uparrow \infty$ as $h \downarrow 0$ might have dynamic solutions. For certain choices of f and g , perhaps the fourth-order term can be sufficiently degenerate to balance the super-diffusivity of the second-order term.

We allow divergences in this paper; we assume our coefficients satisfy:

- $f(y)$ and $g(y)$ are continuous for $y > 0$, but can be singular at $y = 0$.

Next we specify our assumptions on the steady states themselves. For a positive steady state we assume $h \in C^3(\mathbf{R})$. For a touchdown steady state supported on (c, d) , we assume:

- h is C^1 smooth on $[c, d]$ and C^3 smooth on (c, d) .

Thus if the fluid touches down, it does so with an acute contact angle. The higher spatial derivatives might blow up at the contact line. We further assume that:

- if h is a touchdown steady state supported on (c, d) , then the contact angle is the same at both ends. That is, $0 \leq h_x(c) = -h_x(d) < \infty$.

This class of “equal contact angle” touchdown steady states includes zero contact angle steady states. The equal contact angle assumption seems reasonable since a physical droplet in static equilibrium on a horizontal surface has a unique static contact angle, determined by the free energies at the solid/air, solid/liquid and air/liquid interfaces [19].

Outline of the Paper

In Section 2 we present general results for steady states of the evolution equation (1.1). A steady-state solution satisfies the ODE $(f(h)h_{xxx})_x + (g(h)h_x)_x = 0$. We deduce from this that positive periodic steady states and equal contact angle touchdown steady states have a conserved energy $\mathcal{E}(h) = \frac{1}{2}h_x^2 + H(h)$. We then formally construct steady-state solutions via a nonlinear oscillator formulation.

The rest of the paper considers the special case where the coefficients have known power-law behavior at $y = 0$: $f(y) = y^n\Psi(y)$, $g(y) = \mathcal{B}y^m\Psi(y)$, where Ψ is a positive continuous function on $[0, \infty)$ and \mathcal{B} is the Bond number. We rescale the problem to determine universal parameters, one of which is the exponent $q = m - n + 1$.

In Sections 3–4 we show that for such power-law coefficients, the formal construction of solutions in §2 is rigorous. In Section 3, we construct three types of steady states for the long-wave unstable equation ($\mathcal{B} > 0$): positive periodic, touchdown with zero contact angle, and touchdown with nonzero contact angle. In Section 4, we prove the general long-wave stable equation ($\mathcal{B} < 0$) has no nonconstant positive periodic steady states and no touchdown steady states with zero contact angle, and we construct touchdown steady states with nonzero contact angle for the power-law case of f and g .

Section 5 discusses relations between steady states of the rescaled problem and steady

states of the original problem. For periodic steady states we introduce a scale-invariant quantity depending on the period and the volume per period, and use it to answer the question of when the period and volume can be specified, along with similar questions about contact angle, volume and length of touchdown steady states.

In Section 6 we present numerical computations of steady-state solutions, and numerical studies of physically relevant quantities such as the volume and period of the solutions.

Section 7 generalizes a monotonicity result of Schaaf [43] for the period function of the nonlinear oscillator, which helps decide whether the volume and period are monotonic functions of the minimum height of the periodic steady state (for the long-wave unstable equation). We use these monotonicity results in Section 5.

We conclude in Section 8 with a discussion of two open problems: 1) the relation of the scale-invariant quantity to a recent finite-time blow-up conjecture of Bertozzi and Pugh, and 2) the linear stability of steady states and large-time behavior of solutions of the evolution equation.

In Appendices B and C we prove, for general coefficients f and g , that positive bounded steady states are necessarily periodic, and that the only positive periodic traveling wave solution to the evolution equation is the trivial constant one.

Appendix D proves a regularity theorem for the touchdown steady states with zero contact angle (constructed in §3.1.2) of the long-wave unstable equation.

2 Steady states for the general equation

In this section, we prove that both positive periodic steady states and equal contact angle touchdown steady states satisfy a second-order ODE for a nonlinear oscillator.

From the evolution equation (1.1), steady states satisfy a fourth-order ODE that can be integrated once. In §2.1, we prove the resulting integration constant is zero. In §2.2, we integrate once more, resulting in a second-order ODE representing an oscillator with nonlinear restoring force. We then formally derive formulas for the steady states. This nonlinear oscillator formulation is used throughout the article.

2.1 The first integral

A steady-state solution of the evolution equation (1.1) satisfies

$$0 = (f(h)h_{xxx})_x + (g(h)h_x)_x \tag{2.1}$$

on its support, with the support equaling $(-\infty, \infty)$ for a positive periodic steady state and (c, d) for an equal angle touchdown steady state. Integrating (2.1), h satisfies

$$f(h)h_{xxx} + g(h)h_x = C \tag{2.2}$$

for some constant C . In fact:

Theorem 2.1 *For periodic positive steady states and equal contact angle touchdown steady states, $C = 0$.*

The proof, by differential inequalities, is in Appendix A. Similar methods yield the following two theorems, for which we present full statements and proofs in the appendices.

Theorem (*Appendix B*). *For a large class of coefficients f and g , if a steady state h is positive and bounded then it is periodic.*

Hence we are justified in restricting attention to *periodic* positive steady states.

Theorem (*Appendix C*). *The evolution equation (1.1) has no nonconstant positive periodic traveling wave solutions.*

2.2 A nonlinear oscillator formulation

Assume $f(y) > 0$ for all $y > 0$. Theorem 2.1 gives $C = 0$ and so dividing (2.2) by $f(h)$ yields

$$h_{xxx} + F'(h)h_x = 0$$

where $F' = g/f$. This equation holds at all points in \mathbf{R} if h is positive and periodic, and at all points in (c, d) if h is an equal angle touchdown steady state. Integrating, there is a constant D such that

$$h_{xx} + F(h) = D \tag{2.3}$$

on \mathbf{R} (or on (c, d)). Multiplying equation (2.3) by h_x and integrating yields a conserved quantity,

$$\mathcal{E}(h) = \frac{1}{2}h_x^2 + H(h) = \text{const},$$

where $H(y)$ is an antiderivative of $F(y) - D$. Taking x to represent time, the conserved quantity $\mathcal{E}(h)$ is the sum of kinetic energy and potential energy; the solution oscillates in a potential $H(h)$, with nonlinear restoring force $-H'(h)$. The energy $\mathcal{E}(h)$ was first found by Oron and Rosenau [38, 39] for positive periodic steady states, and was used by Novick-Cohen and Peletier to study sign-changing monotonic steady states of Sivashinsky [35] and Cahn–Hilliard [36] equations. For some work on steady states in two dimensions, see [45, 16, 20]. And for an energy minimization approach to a related steady droplet problem with non-acute contact angles, see [34].

We denote the minimum value of h by α , achieved at x_0 , say. If h touches down, then $\alpha = 0$ and we take $x_0 = c$. We determine the value of \mathcal{E} by evaluating at $x = x_0$. For positive periodic steady states this gives

$$\frac{1}{2}h_x(x)^2 + H(h(x)) = H(\alpha)$$

for all x . Touchdown steady states can exist if $H(0)$ is finite; evaluating \mathcal{E} at the contact line yields

$$\frac{1}{2}h_x(x)^2 + H(h(x)) = \frac{1}{2}h_x(c)^2 + H(0) = \frac{1}{2}h_x(c)^2$$

for all $x \in (c, d)$, provided we choose the antiderivative H so that $H(0) = 0$. For later reference, we remark that if $F'(y) = \mathcal{B}y^{q-1}$ for some $\mathcal{B} \neq 0$, then touchdown steady states can only exist when $q > -1$, because otherwise $H(0)$ is infinite.

Solving for the first derivative,

$$\begin{aligned} h_x(x) &= \pm \sqrt{2H(\alpha) - 2H(h(x))} && \text{(positive periodic steady states),} \\ h_x(x) &= \pm \sqrt{h_x(x_0)^2 - 2H(h(x))} && \text{(touchdown steady states).} \end{aligned}$$

Proceeding formally, we invert and then integrate to obtain the inverse function $x = x(h)$ over a half-period. For a positive periodic steady state:

$$x(h) = \frac{1}{\sqrt{2}} \int_{\alpha}^h \frac{dy}{\sqrt{H(\alpha) - H(y)}}. \quad (2.4)$$

Here $h \in [\alpha, \beta]$, where β is the next root bigger than α of $H(y) = H(\alpha)$. If such a root exists then a periodic solution exists. Otherwise, there is no periodic solution. As steady states are invariant under translation, in (2.4) we have taken $x(\alpha) = 0$: h attains its minimum at $x_0 = 0$. The maximum of h is β , and $h_x > 0$ between heights α and β . The complete graph of h is found by reflecting about the half-period point $x(\beta) = P/2$, and then extending periodically.

For a touchdown steady state,

$$x(h) = \int_0^h \frac{dy}{\sqrt{h_x(0)^2 - 2H(y)}} \quad (2.5)$$

where $h \in [0, \beta]$. Again, we have taken $x(0) = 0$, so that h touches down at $c = 0$. In this case, β is the smallest positive root of $2H(y) = h_x(0)^2$. If no such root exists then there is no touchdown steady state with bounded support.

Formula (2.4) holds rigorously if the potential H is strictly convex, and (2.5) holds if H is either strictly convex or concave. The coefficients f and g considered in the rest of the paper have H either convex or concave.

3 Steady states of the long-wave unstable evolution equation — the power law case

We are interested in scale-invariance properties of steady states. For this reason, here and in the rest of the article, we consider coefficient functions f and g with known power-law behavior at $y = 0$:

$$\begin{aligned} f(y) &= y^n \Psi(y) \\ g(y) &= \mathcal{B} y^m \Psi(y) \end{aligned}$$

for exponents $n, m \in \mathbf{R}$, where Ψ is a positive continuous function on $[0, \infty)$. In fact, our results rely only on the ratio g/f , removing Ψ from the problem altogether. The constant $\mathcal{B} \in \mathbf{R}$ is called the *Bond number* — its sign determines whether the equation is long-wave stable ($\mathcal{B} \leq 0$) or long-wave unstable ($\mathcal{B} > 0$), as discussed in the introduction.

In this section we study the long-wave unstable case, $\mathcal{B} > 0$. This case is especially interesting because the evolution equation has interactions between a linearly stabilizing fourth-order term and a linearly destabilizing second-order term.

Introducing

$$q = m - n + 1,$$

we see (in the notation of Section 2) that

$$F'(y) = \frac{g(y)}{f(y)} = \mathcal{B}y^{q-1}, \quad \text{and so} \quad F(y) = \begin{cases} \mathcal{B}y^q/q, & q \neq 0, \\ \mathcal{B} \log y, & q = 0. \end{cases}$$

The steady state satisfies equation (2.3) on its support:

$$h_{xx} + \frac{\mathcal{B}h^q - D}{q} = 0, \quad q \neq 0, \quad (3.1)$$

$$h_{xx} + \mathcal{B} \log h - D = 0, \quad q = 0, \quad (3.2)$$

after replacing D with D/q , when $q \neq 0$. In the rest of this section, we construct and discuss positive periodic steady states (§3.1.1), touchdown steady states with zero contact angle (§3.1.2), and touchdown steady states with nonzero contact angle (§3.2). This variety is to be contrasted with the long-wave stable equation in Section 4, for which we prove there are no nonconstant positive periodic steady states or touchdown steady states with zero contact angle; we do construct touchdown steady states with nonzero contact angle.

We are particularly interested in obtaining formulas for the period/length of each type of steady state, and for the area under each steady state (*i.e.*, the volume of liquid), for two reasons: a) the evolution equation (1.1) conserves volume, and b) the period and area will be important for questions of nonuniqueness of solutions (§5).

Also, we write the steady states in terms of trigonometric and elliptic functions when $q = -\frac{1}{2}, 1, 2$, in §3.1.3.

3.1 Positive periodic steady states and touchdown steady states with zero contact angle

For positive periodic steady states and touchdown steady states with zero contact angle, we first argue that $D > 0$ in equation (3.1), when $q \neq 0$. For $h_{xx} \geq 0$ at some point where $h > 0$, and in the $q > 0$ case, evaluating (3.1) at this point implies $D > 0$. For the $q < 0$ case, evaluating at a maximum point implies that $D > 0$.

Since $\mathcal{B} > 0$ and D is positive for $q \neq 0$, we can rescale the solution h as follows:

$$k(x) = \begin{cases} \left(\frac{\mathcal{B}}{D}\right)^{1/q} h \left(\left(\frac{D}{\mathcal{B}}\right)^{1/2q} \frac{x}{D^{1/2}} \right), & q \neq 0, \\ e^{-D/\mathcal{B}} h \left(\frac{e^{D/2\mathcal{B}}}{\mathcal{B}^{1/2}} x \right), & q = 0. \end{cases} \quad (3.3)$$

The function k satisfies the rescaled equations

$$k_{xx} + \frac{k^q - 1}{q} = 0, \quad q \neq 0, \quad (3.4)$$

$$k_{xx} + \log k = 0, \quad q = 0. \quad (3.5)$$

The rescaling (3.3) is found for $q \neq 0$ by making the ansatz $h(x) = c k(x/d)$ and finding that since $D > 0$, both \mathcal{B} and D can be removed from the problem. The scaling for the $q = 0$ case is then chosen to make the problem continuous in the exponent q .

As solutions are unique up to translation in x , we fix the solution by requiring that

$k = k_\alpha$ attain its minimum height α at $x = 0$: $0 \leq k_\alpha(0) = \alpha \leq 1$, $k'_\alpha(0) = 0$. Plainly $\alpha \leq 1$, by evaluating equation (3.4) or (3.5) at some x with $k_{xx} \geq 0$.

3.1.1 Positive periodic steady states

Both equations (3.4) and (3.5) have the flat solution $k_1(x) \equiv 1$, which we discuss further in §3.1.3. Here, we consider nonconstant positive periodic solutions k_α with minimum heights $\alpha \in (0, 1)$. Define a potential

$$H(y) = \begin{cases} \frac{1}{q} \left[\frac{y^{1+q}}{1+q} - y \right], & q \neq 0, -1, \\ y \log y - y, & q = 0, \\ y - \log y, & q = -1, \end{cases} \quad (3.6)$$

so that $H'(y)$ equals $(y^q - 1)/q$ for $q \neq 0$ and $\log y$ for $q = 0$. We prove:

Theorem 3.1 *For each exponent $q \in \mathbf{R}$ and each $\alpha \in (0, 1)$, there is a smooth positive periodic solution k_α of equations (3.4–3.5) with $k_\alpha(0) = \alpha$ and $k'_\alpha(0) = 0$. This solution has period and area*

$$P_\alpha = \sqrt{2} \int_\alpha^\beta \frac{dk}{\sqrt{H(\alpha) - H(k)}} \quad \text{and} \quad A_\alpha = \sqrt{2} \int_\alpha^\beta \frac{k}{\sqrt{H(\alpha) - H(k)}} dk,$$

where β is the unique solution greater than 1 of $H(\beta) = H(\alpha)$.

The number β exists as claimed because $H(y)$ is strictly convex and has zero slope at $y = 1$.

Proof

We prove the existence of k_α by constructing it. An explicit formula for the inverse is found by viewing the problem as a nonlinear oscillator as in §2.2, with potential function H . We recall equation (2.4) for the inverse function over a half-period,

$$x(k_\alpha) = \frac{1}{\sqrt{2}} \int_\alpha^{k_\alpha} \frac{dk}{\sqrt{H(\alpha) - H(k)}} \quad \text{for } k_\alpha \in [\alpha, \beta]. \quad (3.7)$$

The period of the steady state k_α is $P_\alpha = 2x(\beta)$, and P_α is finite because β is a simple root of $H(y) = H(\alpha)$. The area A_α under a period of $k_\alpha(x)$ is found by integrating the inverse function:

$$A_\alpha = 2 \int_0^{P_\alpha/2} k_\alpha(x) dx = 2 \int_\alpha^\beta k_\alpha \frac{dx}{dk_\alpha} dk_\alpha = \sqrt{2} \int_\alpha^\beta \frac{k}{\sqrt{H(\alpha) - H(k)}} dk.$$

It is clear from the construction that $k_\alpha(x)$ is smooth and satisfies the differential equation (3.4–3.5), except perhaps at its minimum and maximum points. At those points one can show directly (or by using the mean value theorem and the differential equation) that k_α is C^2 -smooth, and then C^∞ -smoothness follows from the equation (3.4–3.5). \square

3.1.2 Touchdown steady states with zero contact angle

In this section, we prove

Theorem 3.1 *For each $q > -1$ there is a touchdown solution $k_0(x)$ of equations (3.4–3.5), with $k_0(0) = 0$ and $k'_0(0) = 0$.*

- (a) *If $q > 0$ then $k_0 \in C^{j,\eta}$ where $j = 1 + \lceil 2q \rceil$ and $\eta = 2 + 2q - (1 + \lceil 2q \rceil) \in (0, 1]$.*
- (b) *If $q = 0$ then $k_0 \in C^{1,\eta}$ for all $\eta \in (0, 1)$.*
- (c) *If $-1 < q < 0$ then $k_0 \in C^{1,\eta}$ where $\eta = (1 - |q|)/(1 + |q|) \in (0, 1)$.*

In the above, $\lceil w \rceil$ denotes the smallest integer larger than or equal to w . For exponents $-1 < q \leq 0$, k_{xx} blows up at the contact line by equations (3.4–3.5), and so $k_0 \notin C^2$. This is consistent with (b) and (c).

In the proof, we present formulas for the solutions $k_0(x)$, and their lengths and areas, in terms of the beta and complementary error functions. These solutions are easily computed using the functions `InverseBetaRegularized` and `InverseErfc` in `Mathematica`. Doing so, we found that for $q > 0$ the zero contact angle condition is apparent when the solutions are viewed on the scale of their length. For negative exponents, the zero contact angle condition is not apparent on this scale — the apparent contact angle is positive. It is only when viewed on a much smaller scale that the zero contact angle condition is visibly satisfied.

Proof

We prove the existence of k_0 by constructing it. We take $h_x(0) = 0$ in equation (2.5) to find the inverse function,

$$x(k_0) = \frac{1}{\sqrt{2}} \int_0^{k_0} \frac{dk}{\sqrt{-H(k)}}. \quad (3.8)$$

Clearly $k_0(0) = 0$ and $k'_0(0) = 0$. The maximum value β of k_0 must satisfy $2H(\beta) = k'_0(0)^2 = 0$, and so definition (3.6) implies $\beta = (1 + q)^{1/q}$ ($= e$ when $q = 0$). (Necessarily $q > -1$ because if $q \leq -1$ then $H(0)$ is infinite and $k_0(x)$ cannot exist with acute contact angles, by §2.2.) As in §3.1.1, k_0 can be shown to be smooth and to satisfy (3.4–3.5) on $(0, P_0)$, where $P_0 = 2x(\beta)$ is the length. We prove in Appendix D that the regularity at the contact line is as stated in (a)–(c).

A formula for the area under $k_0(x)$ follows from integrating the inverse function $x(k_0)$:

$$A_0 = \sqrt{2} \int_0^{(1+q)^{1/q}} \frac{k}{\sqrt{-H(k)}} dk. \quad (3.9)$$

We now present the touchdown steady states $k_0(x)$ with zero contact angle in terms of special functions, for the cases of $q > 0$, $q = 0$, and $-1 < q < 0$ in turn.

- The $q > 0$ case. From (3.8) and the definition of H in (3.6),

$$x(k_0) = \sqrt{\frac{q}{2}} \int_0^{k_0} \frac{dk}{\sqrt{k} \sqrt{1 - k^q/(1 + q)}} \quad (3.10)$$

for $0 < k_0 < \beta = (1+q)^{1/q}$. Changing variables with $\kappa = k^q/(1+q)$ yields

$$x(k_0) = \frac{1}{\sqrt{2q}}(1+q)^{1/2q} \int_0^{\kappa_0} \kappa^{\frac{1}{2q}-1} (1-\kappa)^{\frac{1}{2}-1} d\kappa,$$

where $\kappa_0 = k_0^q/(1+q)$ ranges from 0 to 1. That is,

$$x(k_0) = \frac{1}{\sqrt{2q}}(1+q)^{1/2q} B\left(\kappa_0; \frac{1}{2q}, \frac{1}{2}\right) = \frac{1}{\sqrt{2q}}(1+q)^{1/2q} B\left(\frac{k_0^q}{1+q}; \frac{1}{2q}, \frac{1}{2}\right),$$

where B is the incomplete beta function (formula 6.6.1 in Abramowitz and Stegun [1]).

Thus $k_0(x)$ is given by

$$k_0(x) = (1+q)^{1/q} B^{-1}\left(\sqrt{2q}(1+q)^{-1/2q}x; \frac{1}{2q}, \frac{1}{2}\right)^{1/q},$$

for $0 \leq x \leq P_0/2$. Taking $k_0 = \beta = (1+q)^{1/q}$ determines the length

$$P_0 = \sqrt{\frac{2}{q}}(1+q)^{1/2q} B\left(\frac{1}{2q}, \frac{1}{2}\right).$$

Here $B(\cdot, \cdot)$ denotes the usual beta function (6.2.1 in Abramowitz and Stegun).

The same change of variables in equation (3.9) yields the area of k_0 :

$$A_0 = \sqrt{\frac{2}{q}}(1+q)^{3/2q} B\left(\frac{3}{2q}, \frac{1}{2}\right).$$

- The $q = 0$ case.

$$x(k_0) = \frac{1}{\sqrt{2}} \int_0^{k_0} \frac{dk}{\sqrt{k}\sqrt{1-\log k}}$$

for $0 < k_0 < \beta = e$. Changing variables with $u = \sqrt{1-\log k}/\sqrt{2}$,

$$x(k_0) = 2\sqrt{e} \int_{u_0}^{\infty} e^{-u^2} du, \quad (3.11)$$

where $u_0 = \sqrt{1-\log k_0}/\sqrt{2}$ ranges from 0 to ∞ . Thus

$$x(k_0) = \sqrt{\pi e} \operatorname{erfc}(u_0) = \sqrt{\pi e} \operatorname{erfc}(\sqrt{1-\log k_0}/\sqrt{2}),$$

where erfc is the complementary error function (7.1.2 in Abramowitz and Stegun). Inverting, the steady state is

$$k_0(x) = \exp\left\{1 - 2\left[\operatorname{erfc}^{-1}(x/\sqrt{\pi e})\right]^2\right\}$$

for $0 \leq x \leq \sqrt{\pi e}$. The length and area of k_0 are:

$$P_0 = 4\sqrt{e} \int_0^{\infty} e^{-u^2} du = 2\sqrt{\pi e}, \quad A_0 = 4e^{3/2} \int_0^{\infty} e^{-3u^2} du = 2e^{3/2} \sqrt{\frac{\pi}{3}}.$$

- The $-1 < q < 0$ case. This time, (3.8) and (3.6) yield

$$x(k_0) = \sqrt{\frac{|q|}{2}} \int_0^{k_0} \frac{dk}{\sqrt{k}\sqrt{k^q/(1+q)-1}}, \quad (3.12)$$

where $0 < k_0 < \beta = (1+q)^{1/q}$. Changing variables with $\kappa = (1+q)k^{|q|}$ yields

$$x(k_0) = \frac{1}{\sqrt{2|q|}}(1+q)^{1/2q} \int_0^{\kappa_0} \kappa^{\frac{1}{2|q|}-\frac{1}{2}}(1-\kappa)^{-1/2} d\kappa,$$

where $\kappa_0 = (1+q)k_0^{|q|}$ ranges from 0 to 1. That is,

$$x(k_0) = \frac{1}{\sqrt{2|q|}}(1+q)^{1/2q} B\left(\kappa_0; \frac{1}{2|q|} + \frac{1}{2}, \frac{1}{2}\right) = \frac{1}{\sqrt{2|q|}}(1+q)^{1/2q} B\left(\frac{1+q}{k_0^q}; \frac{1}{2|q|} + \frac{1}{2}, \frac{1}{2}\right).$$

Inverting, the steady state is

$$k_0(x) = (1+q)^{1/q} B^{-1}\left(\sqrt{2|q|}(1+q)^{-1/2q}x; \frac{1}{2|q|} + \frac{1}{2}, \frac{1}{2}\right)^{1/|q|},$$

for $0 \leq x \leq P_0/2$. The length and area are

$$P_0 = \sqrt{\frac{2}{|q|}}(1+q)^{1/2q} B\left(\frac{1}{2|q|} + \frac{1}{2}, \frac{1}{2}\right), \quad A_0 = \sqrt{\frac{2}{|q|}}(1+q)^{3/2q} B\left(\frac{3}{2|q|} + \frac{1}{2}, \frac{1}{2}\right).$$

□

We close by collecting formulas for the product $E_0 = P_0^{3-q}A_0^{q-1}$ that we use in Section 5:

$$E_0 = P_0^{3-q}A_0^{q-1} = \begin{cases} \frac{2}{q}(1+q)B\left(\frac{1}{2q}, \frac{1}{2}\right)^{3-q} B\left(\frac{3}{2q}, \frac{1}{2}\right)^{q-1} & \text{if } q > 0, \\ 4\sqrt{3}\pi & \text{if } q = 0, \\ \frac{2}{|q|}(1+q)B\left(\frac{1}{2|q|} + \frac{1}{2}, \frac{1}{2}\right)^{3-q} B\left(\frac{3}{2|q|} + \frac{1}{2}, \frac{1}{2}\right)^{q-1} & \text{if } -1 < q < 0. \end{cases} \quad (3.13)$$

3.1.3 *Special cases*

We now present special cases for which we have further information.

The constant steady state

To gain insight into the flat steady state $k_1(x) \equiv 1$, we linearize equations (3.4) and (3.5) about $k \equiv 1$. For $1 - \alpha \ll 1$, we write $k_\alpha \approx 1 + v$ where $|v| \ll 1$. For all values of q , the linearization is $v_{xx} + v = 0$. That is, $v(x) = -(1 - \alpha) \cos x$. The period of the linear perturbation is 2π , hence the period P_α of k_α approaches 2π as α approaches 1: $P_\alpha \rightarrow 2\pi$ as $\alpha \rightarrow 1$. This then implies that $A_\alpha \rightarrow 2\pi$ as $\alpha \rightarrow 1$.

We ensure that the problem is continuous in α by assigning period and area

$$P_1 = 2\pi, \quad A_1 = 2\pi,$$

to the flat steady-state, $k_1(x) \equiv 1$.

The trigonometric case: $\mathbf{q} = \mathbf{1}$.

Equation (3.4) becomes linear, $(k - 1)_{xx} + (k - 1) = 0$, with exact solutions

$$k_\alpha(x) = 1 - (1 - \alpha) \cos x.$$

The solutions are positive and periodic if $0 < \alpha < 1$ and are touchdown solutions with zero contact angle if $\alpha = 0$. The period and area are independent of the minimum height: $P_\alpha = 2\pi$ and $A_\alpha = 2\pi$.

The cycloid case: $\mathbf{q} = -1/2$

In this case, the steady states have a parametric representation:

$$\begin{cases} x &= \theta - (1 - \sqrt{\alpha}) \sin \theta, \\ k_\alpha &= [1 - (1 - \sqrt{\alpha}) \cos \theta]^2, \end{cases} \quad \text{for } \theta \in [0, 2\pi]. \quad (3.14)$$

These steady states have a minimum height α , maximum height $\beta = (2 - \sqrt{\alpha})^2$, and period $P_\alpha = 2\pi$. For the touchdown steady state with zero contact angle, $\alpha = 0$, the square root $\sqrt{k_0(x)}$ is a cycloid:

$$\begin{cases} x &= \theta - \sin \theta, \\ \sqrt{k_0} &= 1 - \cos \theta, \end{cases} \quad \text{for } \theta \in [0, 2\pi].$$

To prove all this, we write the potential $H(y)$ in (3.6), with $q = -1/2$, as

$$H(y) = 2(1 - \sqrt{y})^2 - 2.$$

Solving $H(y) = H(\alpha)$ yields $\beta = (2 - \sqrt{\alpha})^2$. The inverse functions (3.7) and (3.8) give

$$x(k_\alpha) = \frac{1}{2} \int_\alpha^{k_\alpha} \left[(1 - \sqrt{\alpha})^2 - (1 - \sqrt{k})^2 \right]^{-1/2} dk, \quad (3.15)$$

for $\alpha \leq k_\alpha \leq \beta = (2 - \sqrt{\alpha})^2$ and all $\alpha \in [0, 1]$. Because $|1 - \sqrt{k}| \leq 1 - \sqrt{\alpha}$, we can define a new parameter

$$\theta = \arccos \frac{1 - \sqrt{k}}{1 - \sqrt{\alpha}},$$

so that θ increases from 0 to π as k increases from α to $\beta = (2 - \sqrt{\alpha})^2$. Substituting $k = [1 - (1 - \sqrt{\alpha}) \cos \theta]^2$ into (3.15) yields $x = \theta_\alpha - (1 - \sqrt{\alpha}) \sin \theta_\alpha$. Writing θ in place of θ_α gives (3.14), for $\theta \in [0, \pi]$. For all minimum heights α , the half-period $P_\alpha/2$ equals π since $x = \pi$ and $k = \beta$ when $\theta = \pi$. We get (3.14) for $\theta \in [\pi, 2\pi]$ by reflection.

The elliptic function case: $\mathbf{q} = 2$

In this case, the steady states can be written in terms of the Jacobian elliptic function sd:

$$k_\alpha(x) = \alpha + 3 \frac{1 - \alpha^2}{\sqrt{12 - 3\alpha^2}} \text{sd} \left(\frac{\sqrt[4]{12 - 3\alpha^2} x}{\sqrt{12}} \middle| m \right)^2$$

where

$$m = \frac{1}{2} - \frac{3\alpha}{2\sqrt{12 - 3\alpha^2}}.$$

Note that $m \in [0, 1/2]$ since $0 \leq \alpha \leq 1$. The differential equation $k_{xx} + (k^2 - 1)/2 = 0$ and the initial conditions $k(0) = \alpha, k'(0) = 0$, are easily verified using properties of sd from Abramowitz and Stegun [1, Ch. 16]. The period is

$$P_\alpha = \frac{\sqrt{12}}{\sqrt[4]{12 - 3\alpha^2}} \cdot 2K(m),$$

where $K(m)$ is the complete elliptic integral of the first kind.

3.2 Touchdown steady states with nonzero contact angles

As the solution is assumed to be C^1 at the contact line, the contact angles are acute. Recall that $f(y) = y^n \Psi(y)$, $g(y) = \mathcal{B}y^m \Psi(y)$ with $\mathcal{B} > 0$ and $q = m - n + 1$. If $q \leq -1$ then §2.2 shows there are no touchdown steady states with acute contact angle. So assume $q > -1$.

Again, we rescale the steady state solution h to simplify the problem. Write

$$S = h_x(0) > 0$$

for the slope of our steady state at the lefthand contact line (taken to be $x = 0$), and let

$$\ell(x) = \left(\frac{\mathcal{B}}{S^2}\right)^{1/(1+q)} h\left(\left(\frac{S^2}{\mathcal{B}}\right)^{1/(1+q)} \frac{x}{S}\right) \quad (3.16)$$

and

$$\delta = \begin{cases} \frac{1}{q} \left(\frac{S^2}{\mathcal{B}}\right)^{1/(1+q)} \frac{D}{S^2}, & q > -1, q \neq 0, \\ \frac{D}{\mathcal{B}} + \log \frac{\mathcal{B}}{S^2}, & q = 0. \end{cases} \quad (3.17)$$

The rescaled versions of equations (3.1) and (3.2) are then

$$\ell_{xx} + \frac{\ell^q}{q} - \delta = 0, \quad q > -1, q \neq 0, \quad (3.18)$$

$$\ell_{xx} + \log \ell - \delta = 0, \quad q = 0, \quad (3.19)$$

with $\ell(0) = 0$, $\ell_x(0) = 1$. For positive exponents $q > 0$, it is clear from equation (3.18) that ℓ is concave if $\delta \leq 0$, whereas ℓ is convex near $\ell = 0$ if $\delta > 0$. Moreover, if $q \leq 0$ then ℓ is convex near $\ell = 0$, for all δ .

The rescaling (3.16–3.17) was found by making the ansatz $\ell(x) = c h(x/d)$. There are three physical quantities, \mathcal{B} , D , and S , and the two rescaling constants can be chosen to reduce the problem to just one parameter. We choose to rescale the contact angle to 45° , $\ell_x(0) = 1$, and choose to rescale the nonlinear terms in equations (3.1) and (3.2) to have coefficients independent of \mathcal{B} . The remaining parameter is δ , which is a function of \mathcal{B} , D , and S .

From the definition of δ , it is clear that for exponents $q \geq 0$, the contact slope $S \rightarrow 0$ as $\delta \rightarrow \infty$, for fixed D . Similarly, for $-1 < q < 0$, the contact slope $S \rightarrow 0$ as $\delta \rightarrow 0$. This suggests that in these limits, the steady states ℓ_δ will have properties related to the zero contact angle solutions k_0 from §3.1.2. In §5.2, we prove that this is true.

We now establish

Theorem 3.2 *For each $q > -1$ and each $\delta \in \mathbf{R}$ (when $q \geq 0$) or $\delta < 0$ (when $-1 < q < 0$), there is a touchdown solution $\ell_\delta(x)$ of the rescaled equation (3.18–3.19) with $\ell_\delta(0) = 0$, $\ell'_\delta(0) = 1$. The length and area are given by*

$$P_\delta = 2 \int_0^{\beta_\delta} \frac{d\ell}{\sqrt{1 - 2L(\ell) + 2\delta\ell}}, \quad A_\delta = 2 \int_0^{\beta_\delta} \frac{\ell}{\sqrt{1 - 2L(\ell) + 2\delta\ell}} d\ell, \quad (3.20)$$

where β_δ and L are defined below.

We do not consider $\delta \geq 0$ when $-1 < q < 0$, for that would imply $\ell_{xx} \geq 0$, preventing ℓ from touching down at two points.

Proof Again, we prove the existence of ℓ_δ by constructing it. The rescaled equations (3.18) and (3.19) can be viewed as nonlinear oscillators with conserved energy

$$\frac{1}{2}\ell_x(x)^2 + L(\ell(x)) - \delta\ell(x) = \frac{1}{2}, \quad (3.21)$$

where we use the boundary condition $\ell_x(0) = 1$ and introduce the function

$$L(y) = \begin{cases} \frac{1}{q(1+q)}y^{1+q}, & q \neq 0, -1, \\ y \log y - y, & q = 0, \\ -\log y, & q = -1. \end{cases} \quad (3.22)$$

Taking $\ell(x) \rightarrow 0$ in (3.21) shows that if $q \leq -1$ then ℓ cannot touch down with finite slope.

Let q and δ be as in the Proposition. The formula (2.5) becomes

$$x(\ell_\delta) = \int_0^{\ell_\delta} \frac{dl}{\sqrt{1 - 2L(\ell) + 2\delta\ell}},$$

which is valid for $\ell_\delta \in [0, \beta_\delta]$, where $\beta_\delta > 0$ is the unique solution of $1 - 2L(y) + 2\delta y = 0$; that such a β_δ exists and is unique is seen as follows. Let $L_1(y) = 1 - 2L(y) + 2\delta y$. Then L_1 is strictly concave, $L_1(0) = 1$ and $L_1(y) \rightarrow -\infty$ as $y \rightarrow \infty$; hence L_1 has a simple root, β_δ .

Because β_δ is simple, $x(\beta_\delta)$ is finite and the inverse $x(\ell_\delta)$ defines a touchdown solution. The formulas for the length P_δ and area A_δ then follow from the inverse function $x(\ell_\delta)$.

It is clear from our construction that the ℓ_δ satisfy (3.18–3.19) and are C^∞ wherever they are positive. They touch down with slope ± 1 at $x = 0$ and $x = P_\delta$. □

3.2.1 Special cases

We now present cases for which we have further information.

The trigonometric case: $\mathbf{q} = 1$

In this case, we solve the rescaled equation (3.18) exactly:

$$\ell_\delta(x) = \frac{\sin \theta + \sin(x - \theta)}{\cos \theta}, \quad 0 < x < 2\theta + \pi,$$

where $\theta = \arctan \delta \in (-\pi/2, \pi/2)$. The length $P_\delta = 2\theta + \pi$ increases from 0 to 2π as θ increases from $-\pi/2$ to $\pi/2$. The area is

$$A_\delta = \int_0^{2\theta+\pi} \ell_\delta(x) dx = (2\theta + \pi) \tan \theta + 2,$$

which increases from 0 to ∞ as θ increases from $-\pi/2$ to $\pi/2$. The product $P_\delta^{3-q} A_\delta^{q-1} = P_\delta^2$ increases from 0 to $4\pi^2$; we use this product in Section 5.

The cycloid case: $\mathbf{q} = -1/2$

In this case, one can obtain solutions related to the cycloid (see §3.1.3). We leave the calculations to the reader.

4 Steady states of the long-wave stable evolution equation

We first prove that the general long-wave stable equation has no nonconstant positive periodic steady states and no touchdown steady states with zero contact angle. We then construct touchdown steady states with nonzero contact angle for the power-law case.

First we consider the general long-wave stable equation, assuming just that $f > 0$ and $g \leq 0$, without assuming f and g behave like power laws. Suppose h were a nonconstant positive periodic steady state, satisfying (2.3). Then $h_{xx}(x_0) > 0$ for some x_0 since h is not concave. Also, F is decreasing since $F' = g/f \leq 0$. Hence $h_{xx}(x) > 0$ whenever $h(x) > h(x_0)$, because $h_{xx}(x_0) = D - F(h(x_0)) > 0$ and F is decreasing. It follows that h is unbounded on one side of x_0 , which is impossible. Thus the only positive periodic steady states are constant. Similarly, all touchdown steady states must be concave, and so must have nonzero contact angles.

We now return to the coefficients with power-law behavior, $f(y) = y^n \Psi(y)$ and $g(y) = \mathcal{B} y^m \Psi(y)$.

We start with the $\mathcal{B} = 0$ case, for which the evolution equation is purely fourth order. From equation (2.3), both positive periodic steady states and equal angle touchdown steady states have constant second derivative on their support. Therefore either $h \equiv \text{const} > 0$ or else

$$h(x) = Sx(1 - x/P), \quad 0 < x < P,$$

where $S > 0$ is the slope at $x = 0$ and $P > 0$ is the length of the droplet. These parabolic steady states are well-known [5, 8, 10, 12, 40]. The area under the droplet is

$$A = \int_0^P Sx(1 - x/P) dx = SP^2/6.$$

Specifying any two of the quantities area, length or contact slope determines the third, uniquely determining the steady state.

We next consider $\mathcal{B} < 0$, the long-wave stable equation with a second-order term. We construct touchdown steady states with nonzero contact angle via a rescaled problem. We proceed as in §3.2, but with a few minor modifications. Again we assume $q > -1$. Write

$$S = h_x(0) > 0$$

for the slope of our steady state at the lefthand contact line, and take

$$\ell(x) = \left(\frac{|\mathcal{B}|}{S^2} \right)^{1/(1+q)} h \left(\left(\frac{S^2}{|\mathcal{B}|} \right)^{1/(1+q)} \frac{x}{S} \right). \quad (4.1)$$

Then ℓ satisfies the rescaled equation

$$\ell_{xx} - \frac{\ell^q}{q} - \delta = 0, \quad q > -1, q \neq 0, \quad (4.2)$$

$$\ell_{xx} - \log \ell - \delta = 0, \quad q = 0, \quad (4.3)$$

where

$$\delta = \begin{cases} \frac{1}{q} \left(\frac{S^2}{|B|} \right)^{1/(1+q)} \frac{D}{S^2}, & q > -1, q \neq 0, \\ \frac{D}{|B|} - \log \frac{|B|}{S^2}, & q = 0. \end{cases}$$

As before, this follows easily from (3.1) and (3.2). Again, ℓ is determined solely by the parameter δ and has slope 1 at $x = 0$. Also, since h is concave, ℓ is concave.

For $q > -1$, define

$$\delta(q) = \begin{cases} -\frac{1}{q} \left(\frac{1+q}{2} \right)^{q/(1+q)}, & q > -1, q \neq 0, \\ \log 2, & q = 0. \end{cases}$$

We prove

Theorem 4.1 *For each $q > -1$ and each $\delta < \delta(q)$ there is a touchdown solution ℓ_δ of the rescaled equation (4.2–4.3) with $\ell_\delta(0) = 0$, $\ell'_\delta(0) = 1$. The solution has length and area*

$$P_\delta = 2 \int_0^{\beta_\delta} \frac{d\ell}{\sqrt{1 + 2L(\ell) + 2\delta\ell}}, \quad A_\delta = 2 \int_0^{\beta_\delta} \frac{\ell}{\sqrt{1 + 2L(\ell) + 2\delta\ell}} d\ell, \quad (4.4)$$

where L was defined in (3.22) and β_δ is defined below.

If $\delta \geq \delta(q)$ then there is no touchdown solution with bounded support: ℓ_δ still exists but cannot touch down at two points.

Proof As before, there is a conserved quantity which we evaluate at the contact line,

$$\frac{1}{2} \ell_x(x)^2 - L(\ell(x)) - \delta\ell(x) = \frac{1}{2}.$$

The inverse of the solution over a half-period is

$$x(\ell_\delta) = \int_0^{\ell_\delta} \frac{d\ell}{\sqrt{1 + 2L(\ell) + 2\delta\ell}}. \quad (4.5)$$

This formula is valid for $\ell_\delta \in [0, \beta_\delta]$, where $\beta_\delta > 0$ is the smallest solution of $1 + 2L(y) + 2\delta y = 0$; that such a β_δ exists is seen as follows. Writing $L_1(y) = 1 + 2L(y) + 2\delta y$, one sees that L_1 is strictly convex and $L_1(0) = 1$. It suffices to show L_1 is somewhere negative, since then the equation $L_1(y) = 0$ has a smallest root β_δ and this root is simple — hence $x(\beta_\delta)$ is finite. For $q = 0$: the minimum of L_1 is at $e^{-\delta}$ because $L'_1(e^{-\delta}) = 0$, and $L_1(e^{-\delta}) < 0$ since $\delta < \delta(0) = \log 2$. For other values of $q > -1$, argue similarly.

Because $x(\beta_\delta)$ is finite, the inverse $x(\ell_\delta)$ defines a touchdown solution. The formulas for the length P_δ and area A_δ then follow from the inverse function $x(\ell_\delta)$.

Our construction implies the ℓ_δ satisfy (4.2–4.3) and are C^∞ wherever they are positive. They touch down with slope ± 1 at $x = 0$ and $x = P_\delta$.

□

The Hyperbolic Trigonometric Case: $\mathbf{q} = \mathbf{1}$

In this case, the rescaled equation (4.2) is $(\ell + \delta)_{xx} - (\ell + \delta) = 0$ with $\ell(0) = 0$, $\ell_x(0) = 1$, where δ is fixed. The upper bound on δ is $\delta < \delta(1) = -1$. The exact solution is

$$\ell_\delta(x) = \frac{\cosh \gamma - \cosh(x - \gamma)}{\sinh \gamma}, \quad 0 < x < 2\gamma,$$

where $\coth(\gamma) = -\delta$. Since γ increases from 0 to ∞ as δ increases from $-\infty$ to -1 , the length $P_\delta = 2\gamma$ increases from 0 to ∞ . The area is

$$A_\delta = \int_0^{2\gamma} \ell_\delta(x) dx = 2\gamma \coth \gamma - 2,$$

which increases from 0 to ∞ as γ increases from 0 to ∞ . Furthermore, the mean value $A_\delta/P_\delta = \coth \gamma - 1/\gamma$ increases with γ .

5 The power-law case — specifying the period, area and contact angle

Can one specify both the period and area of a positive periodic steady state? If so, is the steady state unique? More precisely, fix the physical parameters m and n and the Bond number \mathcal{B} . Given positive numbers P and A , the question is whether a constant $D > 0$ exists such that the steady-state equation $h_{xx} + (\mathcal{B}h^q - D)/q = 0$ has a positive periodic solution with period P and area A . Similarly, for touchdown steady states we ask whether one can specify any two of the quantities length, area and contact angle and be guaranteed a solution. And when is the solution unique?

We address these questions in three subsections:

§5.1 The long-wave unstable equation — positive periodic steady states and touchdown steady states with zero contact angle.

§5.2 The long-wave unstable equation — touchdown steady states with nonzero contact angle.

§5.3 The long-wave stable equation.

As in Sections 3 and 4, we work with coefficient functions $f(y) = y^n \Psi(y)$ and $g(y) = \mathcal{B}y^m \Psi(y)$, where Ψ is a positive continuous function on $[0, \infty)$. Recall that $q = m - n + 1$.

5.1 The long-wave unstable equation — positive periodic steady states and touchdown steady states with zero contact angle.

Here $\mathcal{B} > 0$. We constructed positive periodic steady states in §3.1.1 and touchdown steady states with zero contact angle in §3.1.2. This involved rescaling h to k_α , where k_α has minimum value α , period P_α and area A_α . We recall from §3 that steady states

can touch down only when $q > -1$. To state our results, we introduce

$$E_\alpha = P_\alpha^{3-q} A_\alpha^{q-1} \quad \text{for } \alpha \in [0, 1],$$

with the convention that $E_0 = 0$ when $q \leq -1$. Then $E_1 = 4\pi^2$ by §3.1.3, and $E_0 = P_0^{3-q} A_0^{q-1}$ was calculated in terms of beta functions in (3.13), for $q > -1$.

The attainable values of period and area for h are determined by the range of E_α . Specifically, let $P, A > 0$. Then:

Analytical claims about the existence of steady states

5.1.1. A nonconstant positive periodic steady state with period P and area A exists if and only if $\mathcal{B}P^{3-q}A^{q-1} = E_\alpha$ for some $\alpha \in (0, 1)$.

5.1.2. A touchdown steady state with zero contact angle, period P and area A exists if and only if $q > -1$ and $\mathcal{B}P^{3-q}A^{q-1} = E_0$. This steady state is unique up to translation.

The attainable periods and areas are therefore severely constrained when $q > -1$, since E_α has bounded range and this range is bounded away from 0, by continuity in α .

Proof Proof of Claims 5.1.1–5.1.2.

Denote the periods and areas for h and k_α by P_h, A_h and P_α, A_α respectively. The rescaling (3.3) implies

$$P_\alpha = \begin{cases} \left(\frac{\mathcal{B}}{D}\right)^{1/2q} D^{1/2} P_h, & q \neq 0, \\ e^{-D/2\mathcal{B}} \mathcal{B}^{1/2} P_h, & q = 0, \end{cases} \quad \text{and} \quad A_\alpha = \begin{cases} \left(\frac{\mathcal{B}}{D}\right)^{3/2q} D^{1/2} A_h, & q \neq 0, \\ e^{-3D/2\mathcal{B}} \mathcal{B}^{1/2} A_h, & q = 0, \end{cases} \quad (5.1)$$

therefore the product $P_h^{3-q} A_h^{q-1}$ is essentially invariant under rescaling:

$$\mathcal{B}P_h^{3-q} A_h^{q-1} = P_\alpha^{3-q} A_\alpha^{q-1} = E_\alpha. \quad (5.2)$$

Note that h touches down if and only if k_α does, which happens when $\alpha = 0$.

The “only if” directions of the claims follow immediately from this invariance relation (5.2). For the “if” directions, first choose α such that $E_\alpha = \mathcal{B}P^{3-q}A^{q-1}$. Now that α is known, k_α, P_α and A_α are known. Then set $P_h = P, A_h = A$, and determine D from the scaling relations in (5.1). Once D is known, k_α determines h via the rescaling (3.3). This proves the claims, and shows how to construct a steady state with specified values of the period and area. □

The range of E_α is indicated by the shaded regions in Figure 4, and was found by the numerical and analytical work described in Sections 6 and 7. In the figure we write $q^* \approx 1.768$ for one solution of $E_0(q^*) = 4\pi^2$ (the other solution is $q = 1$), and we use the notation

$$E_0(q) = E_0 \quad \text{and} \quad E_{min}(q) = \min_\alpha E_\alpha$$

to emphasize the q -dependence. From Figure 4, $E_{max}(q) = E_0(q)$ or $4\pi^2$ for all q and

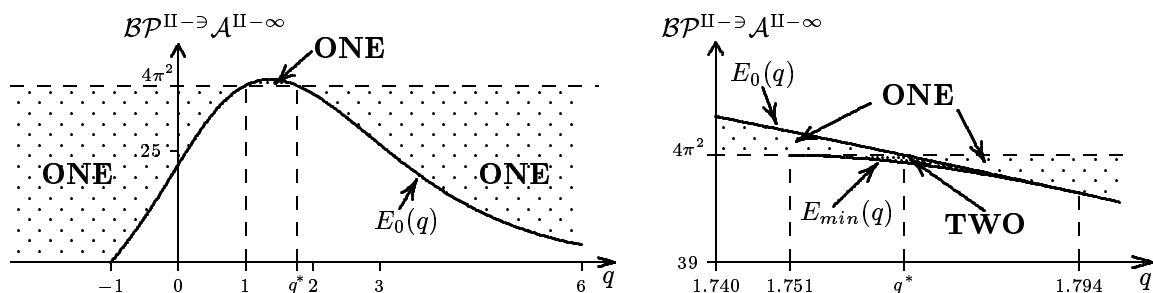


FIGURE 4. Number of periodic steady states with period P and area A ; close-up on right.

$E_{\min}(q)$ equals either $E_0(q)$ or $4\pi^2$, except when $1.750 < q < 1.795$ (approx.); remember for $q \leq -1$ that $E_0(q) = 0$ by definition.

Referring to the figures, we now answer the question of how many positive periodic steady states there can be with a given period and area.

Analytical and numerical claims about uniqueness

5.1.3. [N] A nonconstant positive periodic steady state with period P and area A exists if and only if

$$\begin{cases} E_0(q) < \mathcal{BP}^{3-q} A^{q-1} < 4\pi^2, & \text{when } q < 1 \text{ or } q \geq 1.795, \\ E_0(q) > \mathcal{BP}^{3-q} A^{q-1} > 4\pi^2, & \text{when } 1 < q \leq 1.750, \end{cases}$$

and this steady state is unique up to translation. We prove this claim for exponents $-1/2 \leq q < 1$ and $3 \leq q \leq 4.54$.

5.1.4. [N] Suppose $1.751 \leq q \leq q^*$. A nonconstant positive periodic steady state with period P and area A exists if and only if $E_{\min}(q) \leq \mathcal{BP}^{3-q} A^{q-1} < E_0(q)$. There are two such steady states up to translation if $E_{\min}(q) < \mathcal{BP}^{3-q} A^{q-1} < 4\pi^2$, and otherwise there is just one.

5.1.5. [N] Suppose $q^* \leq q \leq 1.794$. A nonconstant positive periodic steady state with period P and area A exists if and only if $E_{\min}(q) \leq \mathcal{BP}^{3-q} A^{q-1} < 4\pi^2$. There are two such steady states up to translation if $E_{\min}(q) < \mathcal{BP}^{3-q} A^{q-1} < E_0(q)$, and otherwise there is just one.

Here and in the rest of this section, a label “N” indicates we have numerical evidence (and sometimes a partial proof) for the statement. We do prove 5.1.3 completely for some q -values.

In these claims we omit the “trigonometric” case $q = 1$, which is easily treated like in §3.1.3. One finds the period is fixed at $2\pi/\sqrt{\mathcal{B}}$ but the area is arbitrary.

Proof Evidence for Claims 5.1.3–5.1.5.

For $q < 1$ and $q \geq 1.795$, Claim 5.1.3 follows from 5.1.1 provided E_α is strictly increasing; we numerically show this monotonicity in §6.1. In fact, we prove E_α is strictly increasing for $-1/2 \leq q < 1$ and $3 \leq q \leq 4.54$: see Theorem 7.2 in §7.2. For the uniqueness claim in 5.1.3, observe that if E_α is strictly monotonic then the requirement $\mathcal{BP}^{3-q} A^{q-1} = E_\alpha$ uniquely determines α , and the construction in the proof of 5.1.1 then

shows that α determines h . The value 1.795 above is a numerical approximation of an exact critical exponent lying between 1.794 and 1.795. Also, note that we only considered q between -4 and 10 in our numerical studies. We believe the monotonicity phenomena persist beyond that range.

For $1 < q \leq 1.750$, we argue similarly, using the numerical result from §6.1 that E_α is strictly decreasing when $1 < q \leq 1.750$. Again, 1.750 is a numerical approximation of an exact critical exponent between 1.750 and 1.751. This finishes Claim 5.1.3.

Claims 5.1.4 and 5.1.5 are based on the following numerical observation from §6.1. When $1.751 \leq q \leq 1.794$, E_α initially decreases and then increases, as a function of α . Hence a horizontal line will cut the graph of E_α for $0 < \alpha < 1$ precisely twice at heights between E_{min} and $\min\{E_0, E_1 = 4\pi^2\}$, and at most once at all other heights. In the former case, if we choose P and A such that $\mathcal{B}P^{3-q}A^{q-1} = E_{\alpha_1} = E_{\alpha_2}$ for some distinct $\alpha_1, \alpha_2 \in (0, 1)$, then we can use k_{α_1} and k_{α_2} to construct two different nonconstant positive steady states with period P and area A . We show such a pair of steady states in Figure 2, as constructed numerically at the end of §6.1. \square

Incidentally, VanHook et al. [47] use the nonlinear oscillator formulation, $\mathcal{E}(h) = \frac{1}{2}h_x^2 + H(h)$, to consider a thin film with thermocapillary and gravitational effects. They numerically study positive periodic steady states with fixed mass, $A = 2\pi$, and period, $P = 2\pi/k$, where k is an integer. Their potential H is especially interesting in that it is non-convex.

We close this subsection with a comment on what aspects of the evolution equation can be determined from its steady states. Assume one has a fluid, a surface, and a gas such that a reasonable modeling evolution equation has coefficients $f(y) = ay^n\Psi(y)$ and $g(y) = by^m\Psi(y)$.

Assume further that we have a pair of touchdown steady-state solutions, uniform in the y -direction and with zero contact angle. Write P and \hat{P} for the lengths of the two steady states, and A and \hat{A} for their areas. These two solutions must rescale to the same function k_0 .

By the invariance relation (5.2), $\mathcal{B}P^{3-q}A^{q-1} = P_0(q)^{3-q}A_0(q)^{q-1} = \mathcal{B}\hat{P}^{3-q}\hat{A}^{q-1}$, where we have written $P_0(q)$ and $A_0(q)$ for the length and area of the rescaled solution k_0 . Solving, we find

$$m - n = q - 1 = 2 \frac{\log(P/\hat{P})}{\log(\hat{A}P/A\hat{P})}, \quad \text{and} \quad \mathcal{B} = \frac{P_0(q)^{3-q}A_0(q)^{q-1}}{P^{3-q}A^{q-1}}.$$

Thus one can determine the difference of exponents $m - n$ and the Bond number \mathcal{B} solely from measurements of volume and length for two distinct touchdown steady states with zero contact angle.

5.2 The long-wave unstable equation — touchdown steady states with nonzero contact angle.

Again $\mathcal{B} > 0$. Consider a touchdown steady state h with nonzero contact angle, translated so its lefthand end sits at $x = 0$. Can we arbitrarily specify any two of its length, area

and contact slope? And is it unique? (Because the steady states are fixed at $x = 0$, in the following “unique” is the same as “unique up to translation”.)

For the claims below labeled “N” we have numerical evidence and partial proofs; we prove all the other parts. The positive numbers $P_{max}(q)$, $A_{max}(q)$ and $E_{max}(q)$ mentioned in these results are defined later, and the quantity $E_{\alpha=0}(q)$ is known in terms of beta functions by (3.13). Figure 5 represents the claims graphically.

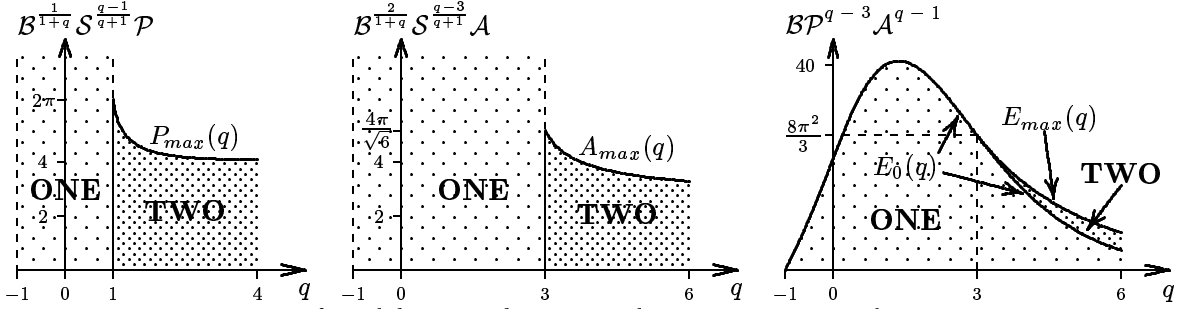


FIGURE 5. Number of touchdown steady states with nonzero contact angle with given: P and S ; A and S ; P and A .

Analytical and numerical claims about existence and uniqueness of steady states

5.2.1. Consider touchdown steady states with length P and slope S .

- If $-1 < q < 1$ then a unique such steady state exists.
- If $q = 1$ then such a steady state exists if and only if $\mathcal{B}^{1/2}P < 2\pi$, and it is unique.
- [N] Let $q > 1$. Then there are two, one or zero such steady states, according to whether $\mathcal{B}^{1/(q+1)}S^{(q-1)/(q+1)}P$ is less than, equal to, or greater than $P_{max}(q)$, respectively.

5.2.2. Consider touchdown steady states with area A and slope S .

- If $-1 < q < 3$ then a unique such steady state exists.
- If $q = 3$ then such a steady state exists if and only if $\mathcal{B}^{1/2}A < 4\pi/\sqrt{6}$, and it is unique.
- [N] Let $q > 3$. Then there are two, one or zero such steady states, according to whether $\mathcal{B}^{2/(q+1)}S^{(q-3)/(q+1)}A$ is less than, equal to, or greater than $A_{max}(q)$, respectively.

5.2.3. Consider touchdown steady states with length P and area A .

- [N] If $-1 < q < 1$ then such a such steady state exists if and only if $\mathcal{B}P^{3-q}A^{q-1} < E_{\alpha=0}(q)$, and it is unique.
- If $1 \leq q \leq 3$ then such a such steady state exists if and only if $\mathcal{B}P^{3-q}A^{q-1} < E_{\alpha=0}(q)$, and it is unique. Note that $E_{\alpha=0}(3) = 8\pi^2/3$.
- [N] Let $q > 3$. Then there are two, one or zero such steady states, de-

pending on the value of $\mathcal{B}P^{3-q}A^{q-1}$: one if $\mathcal{B}P^{3-q}A^{q-1} \leq E_{\alpha=0}(q)$, two if $E_{\alpha=0}(q) < \mathcal{B}P^{3-q}A^{q-1} < E_{max}(q)$, one if $\mathcal{B}P^{3-q}A^{q-1} = E_{max}(q)$, and none if $\mathcal{B}P^{3-q}A^{q-1} > E_{max}(q)$.

We have not considered $q \leq -1$ in these claims because steady states can touch down with finite slope only when $q > -1$.

We justify these claims by rescaling h to ℓ_δ , the solution constructed in §3.2. From (3.16),

$$P_\delta = \mathcal{B}^{1/(q+1)} S_h^{(q-1)/(q+1)} P_h \quad \text{and} \quad A_\delta = \mathcal{B}^{2/(q+1)} S_h^{(q-3)/(q+1)} A_h, \quad (5.3)$$

where we denote the length, area and slope at the contact line for h and ℓ_δ by P_h , A_h , S_h and P_δ , A_δ , S_δ respectively, with $S_\delta = 1$. The product $P_h^{3-q} A_h^{q-1}$ is essentially invariant:

$$P_\delta^{3-q} A_\delta^{q-1} = \mathcal{B} P_h^{3-q} A_h^{q-1}. \quad (5.4)$$

Recalling from §3.2 that a solution ℓ_δ exists if and only if $\delta \in \mathbf{R}$ (when $q \geq 0$) or $\delta < 0$ (when $-1 < q < 0$), we define

$$E_\delta = P_\delta^{3-q} A_\delta^{q-1} \quad \text{for } \delta \in \mathbf{R} \text{ (when } q \geq 0) \text{ or } \delta < 0 \text{ (when } -1 < q < 0).$$

We will obtain Claims 5.2.1–5.2.3 from the following Results (i)–(iii) about P_δ , A_δ , and E_δ as functions of δ , illustrated in Figure 6. Note that in addressing Result (i) we prove P_δ attains a finite maximum value when $q > 1$, and similarly in Result (ii) for A_δ when $q > 3$; we denote these maximum values by $P_{max}(q)$ and $A_{max}(q)$. For E we prove E_δ is bounded; numerical evidence suggests that when $q > 3$, E_δ attains a maximum value $E_{max}(q)$.

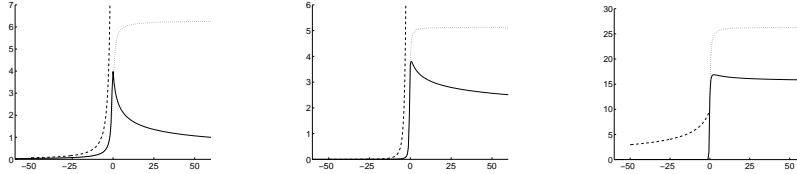


FIGURE 6. L to R: P_δ ($q = -0.5, 1, 4$), A_δ ($q = -0.5, 3, 4$), E_δ ($q = -0.5, 3, 4$). Curves are dashed, dotted, solid with increasing q .

Analytical and numerical results about P_δ , A_δ , and E_δ

- (i) P_δ : If $-1 < q < 1$ then P_δ increases strictly from 0 to ∞ .
If $q = 1$ then P_δ increases strictly from 0 to 2π .
[N] If $q > 1$ then P_δ increases strictly from 0 to $P_{max}(q)$ and then decreases strictly to 0.
- (ii) A_δ : If $-1 < q < 3$ then A_δ increases strictly from 0 to ∞ .
If $q = 3$ then A_δ increases strictly from 0 to $4\pi/\sqrt{6}$.
[N] If $q > 3$ then A_δ increases strictly from 0 to $A_{max}(q)$ and then decreases strictly to 0.
- (iii) E_δ : [N] If $-1 < q < 1$ then E_δ increases strictly from 0 to $E_{\alpha=0}(q)$.
If $1 \leq q \leq 3$ then E_δ increases strictly from 0 to $E_{\alpha=0}(q)$.

[N] If $q > 3$ then E_δ increases strictly from 0 to $E_{max}(q)$ and then decreases strictly to $E_{\alpha=0}(q)$.

Again, for the results labeled “N” we prove some parts and provide numerical evidence for the rest.

Proof Results (i) and (ii): the Period and Area. Recall from §3.2 that β_δ , the maximum value of ℓ_δ , is the unique positive solution of the equation

$$-1 + 2L(y) = 2\delta y. \quad (5.5)$$

Observe that β_δ is a continuous, strictly increasing function of δ that approaches 0 as $\delta \rightarrow -\infty$, since the lefthand side of equation (5.5) is strictly convex and the righthand side is linear in y , with the left-hand side equaling -1 and the righthand side equaling 0 when $y = 0$. Also $\beta_\delta \rightarrow \infty$ as $\delta \rightarrow \infty$ (when $q \geq 0$) or as $\delta \rightarrow 0$ (when $-1 < q < 0$).

By changing variable with $\ell = \beta_\delta u$ in the formulas (3.20) for the period and area, and then using that $2\delta\beta_\delta = -1 + 2L(\beta_\delta)$, we get for $q \neq 0$ that

$$P_\delta = 2 \int_0^1 \left[1 + \beta_\delta^{1+q} \frac{2u}{q(1+q)} \frac{1-u^q}{1-u} \right]^{-1/2} \frac{du}{\sqrt{1-u}} \cdot \beta_\delta \quad (5.6)$$

$$= 2 \int_0^1 \left[\beta_\delta^{-1-q} + \frac{2u}{q(1+q)} \frac{1-u^q}{1-u} \right]^{-1/2} \frac{du}{\sqrt{1-u}} \cdot \beta_\delta^{(1-q)/2}, \quad (5.7)$$

$$A_\delta = 2 \int_0^1 \left[1 + \beta_\delta^{1+q} \frac{2u}{q(1+q)} \frac{1-u^q}{1-u} \right]^{-1/2} \frac{u du}{\sqrt{1-u}} \cdot \beta_\delta^2 \quad (5.8)$$

$$= 2 \int_0^1 \left[\beta_\delta^{-1-q} + \frac{2u}{q(1+q)} \frac{1-u^q}{1-u} \right]^{-1/2} \frac{u du}{\sqrt{1-u}} \cdot \beta_\delta^{(3-q)/2}. \quad (5.9)$$

If $q = 0$ then the same formulas hold, except with $(1-u^q)/q$ replaced by $\log(1/u)$. In the above, we have written each integrand as a positive continuous function on $[0, 1]$ multiplied by the divergent factor $1/\sqrt{1-u}$.

For all $q > -1$, equations (5.6) and (5.8) show P_δ and A_δ approach 0 as $\delta \rightarrow -\infty$ (that is, as $\beta_\delta \rightarrow 0$).

Equation (5.7) shows P_δ increases strictly as δ (and hence β_δ) increases, provided $-1 < q \leq 1$. Similarly A_δ increases strictly if $-1 < q \leq 3$, by (5.9). Clearly P_δ increases to ∞ if $-1 < q < 1$, as does A_δ if $-1 < q < 3$. For $q = 1$ we have $\lim_{\delta \rightarrow \infty} P_\delta = 2\pi$ by §3.2.1, and for $q = 3$ we compute from (5.9) that

$$\lim_{\delta \rightarrow \infty} A_\delta = 2\sqrt{6} \int_0^1 (1-u^3)^{-1/2} u^{1/2} du = 4\pi/\sqrt{6},$$

by putting $u = (\sin \theta)^{2/3}$. For $q > 1$ we see from (5.7) that P_δ approaches 0 as $\delta \rightarrow \infty$, and so $P_{max}(q)$ is attained. Similarly for $q > 3$, (5.9) shows $A_\delta \rightarrow 0$ as $\delta \rightarrow \infty$ and so $A_{max}(q)$ is attained.

We have proved all of Results (i) and (ii) except for the claim that when $q > 1$, P_δ first increases strictly to its maximum and then decreases, and similarly for A_δ when $q > 3$. For these we present numerical evidence in §6.2. \square

Proof Result (iii): the Product E .

Using (5.6) and (5.8) gives $E_\delta = P_\delta^{3-q} A_\delta^{q-1} \rightarrow 0$ as $\delta \rightarrow -\infty$ (i.e., as $\beta_\delta \rightarrow 0$). Using (5.7) and (5.9) shows that

$$E_\delta = P_\delta^{3-q} A_\delta^{q-1} = 4 \left(\int_0^1 \left[\beta_\delta^{-1-q} + \frac{2u}{q(1+q)} \frac{1-u^q}{1-u} \right]^{-1/2} (1-u)^{-1/2} du \right)^{3-q} \left(\int_0^1 \left[\beta_\delta^{-1-q} + \frac{2u}{q(1+q)} \frac{1-u^q}{1-u} \right]^{-1/2} (1-u)^{-1/2} u du \right)^{q-1} \quad (5.10)$$

Hence

$$E_\delta \rightarrow 2(1+q) \left(\int_0^1 [(1-u^q)/q]^{-1/2} u^{-1/2} du \right)^{3-q} \left(\int_0^1 [(1-u^q)/q]^{-1/2} u^{1/2} du \right)^{q-1}$$

as $\beta_\delta \rightarrow \infty$. This last quantity equals $E_{\alpha=0}(q)$ by substituting $v = u^{|q|}$ when $q \neq 0$ (or $u = \exp(-2v^2)$ when $q = 0$) and using beta functions as in §3.1.2. The appearance of $E_{\alpha=0}$ here is not surprising: for $q > 0$, letting $\delta \rightarrow \infty$ in (3.17) is roughly equivalent to taking $S_h \rightarrow 0$, and $S_h = 0$ corresponds to a touchdown solution with zero contact angle, namely k_α with $\alpha = 0$.

Observe that E_δ is bounded since E_δ approaches finite limits as $\delta \rightarrow \pm\infty$.

From (5.10) we also deduce that E_δ is a strictly increasing function of δ , when $1 \leq q \leq 3$.

We have proved all of Result (iii) except for the claim that when $-1 < q < 1$, E_δ is strictly increasing, and that when $q > 3$, E_δ first increases and then decreases. For these we present numerical evidence in §6.2. \square

Proof Justification of Claims 5.2.1–5.2.3.

For 5.2.1, suppose we are given positive numbers P and S . Substituting $P_h = P$ and $S_h = S$ into the first of the rescaling relations in (5.3) determines the righthand side of $P_\delta = \mathcal{B}^{1/(q+1)} S^{(q-1)/(q+1)} P$. Thus the question becomes, “Is there a value of δ for which $P_\delta = \text{RHS}$, and can there be more than one?” Once we know δ , we can invert the rescaling and express h in terms of ℓ_δ ; clearly h then has length P and touchdown slope S , and different values of δ will yield different steady states h . The first claim therefore follows directly from the monotonicity properties of P_δ in Result (i) above.

For 5.2.2, we use the second of the rescaling relations in (5.3) and argue similarly, using Result (ii) for A_δ .

For 5.2.3, suppose we are given positive numbers P and A . Substitute $P_h = P$ and $A_h = A$ into (5.4), hence determining the desired value of $E_\delta = P_\delta^{3-q} A_\delta^{q-1}$. Once we know δ , we determine S_h by substituting $P_h = P$, $A_h = A$ into (5.3). Then we can invert the rescaling and express h in terms of ℓ_δ , and h has length P and area A . The third claim thus follows directly from the monotonicity properties of E_δ in Result (iii) above. \square

We have seen in this section that for steady states of the long-wave unstable evolution equation, the attainable periods, lengths, volumes and contact angles are constrained by certain inequality relations.

A similar example of a length-determined volume constraint is found in the work of Tuck and Schwartz [46] on thin droplets on a vertical surface. They explicitly solve for the thickness $h(y)$ of the steady state:

$$h(y) = \frac{y(L-y)}{12L^3\sigma}(L^4\rho g + 72V\sigma - 2L^3\rho g y),$$

where L is the length of the drop ($y = L$ at the upper end, $y = 0$ at the bottom), V is the volume, ρ is the fluid density, g is the gravitational constant, and σ is the surface tension constant. Necessarily $h'(L) \leq 0$, which implies $V \geq L^4\rho g/(72\sigma)$. In this way, the length L constrains the volume V . Tuck and Schwartz also performed interesting numerical studies of the evolution equation, where they chose initial data whose volume was too small for there to be any steady state to which the solution could converge in the infinite-time limit. We plan to carry out similar studies for the evolution equation (1.1) in a future article.

5.3 The long-wave stable equation.

We now take $\mathcal{B} \leq 0$. We first consider the case where $\mathcal{B} = 0$ and the evolution equation is purely fourth order, $h_t = -(f(h)h_{xxx})_x$. We presented an exact formula for h in §4, from which it follows that specifying any two of the (positive) quantities length, area and slope uniquely determines the third via the relation $6A = SP^2$. Clearly there does exist a touchdown steady state with these values.

We now turn to the $\mathcal{B} < 0$ case, the long-wave stable equation with a second-order term. From §4, there are no positive periodic steady states or zero contact angle touchdown steady states. If $q > -1$ then there are touchdown solutions h with nonzero contact slope $S = h_x(0) > 0$ at $x = 0$. For such steady states we claim:

Analytical and numerical claims about existence and uniqueness of steady states

5.3.1. Given $P, S > 0$, there is a unique steady state with that length and slope.

5.3.2. Given $A, S > 0$, there is a unique steady state with that area and slope.

5.3.3. Given $P, A > 0$, there is a steady state with that length and area. The steady state is unique, if $q \geq 1$, and numerical work suggests the solution is unique for $-1 < q < 1$ also.

We justify these claims by rescaling h to ℓ_δ , the solution constructed in §4. We write the length, area and contact slope for h and ℓ_δ as P_h, A_h, S_h and $P_\delta, A_\delta, S_\delta$ respectively, with $S_\delta = 1$. The rescaling (4.1) determines

$$P_\delta = |\mathcal{B}|^{1/(q+1)} S_h^{(q-1)/(q+1)} P_h \quad \text{and} \quad A_\delta = |\mathcal{B}|^{2/(q+1)} S_h^{(q-3)/(q+1)} A_h. \quad (5.11)$$

The product $P_h^{3-q} A_h^{q-1}$ is essentially invariant under the rescaling that takes h to ℓ_δ :

$$P_\delta^{3-q} A_\delta^{q-1} = |\mathcal{B}| P_h^{3-q} A_h^{q-1}. \quad (5.12)$$

Recall from §4 that a solution ℓ_δ exists if and only if $\delta < \delta(q)$. Define

$$E_\delta = P_\delta^{3-q} A_\delta^{q-1} \quad \text{for } \delta < \delta(q).$$

We later obtain Claims 5.3.1–5.3.3 from the following results about P_δ, A_δ , and E_δ as

functions of δ . We do not completely prove Result (iv), though we support it analytically and numerically.

Analytical and numerical results about P_δ , A_δ , and E_δ

- (i) P_δ : If $q > -1$ then P_δ increases strictly from 0 to ∞ .
- (ii) A_δ : If $q > -1$ then A_δ increases strictly from 0 to ∞ .
- (iii) E_δ : If $q \geq 1$ then E_δ increases strictly from 0 to ∞ .
- (iv) E_δ : [N] If $1 > q > -1$ then E_δ increases strictly from 0 to ∞ .

In §4, we proved all these claims for the exponent $q = 1$. (Note that $E_\delta = P_\delta^2$ when $q = 1$.)

Proof Proof of Results (i) and (ii).

Recall from §4 that β_δ , the maximum value of ℓ_δ , is the first positive solution of the equation

$$-1 - 2L(y) = 2\delta y. \quad (5.13)$$

Observe that β_δ is a continuous, strictly increasing function of δ that approaches 0 as $\delta \rightarrow -\infty$, since the lefthand side of equation (5.13) is strictly concave and the righthand side is linear in y , with the lefthand side equaling -1 and the righthand side equaling 0 when $y = 0$. As $\delta \rightarrow \delta(q)$,

$$\beta_\delta \rightarrow \beta_{\delta(q)} = \left(\frac{1+q}{2} \right)^{\frac{1}{1+q}}.$$

Note that $1 + 2L(y) + 2\delta(q)y$ has a double root at $y = \beta_{\delta(q)}$.

Changing variables with $\ell = \beta_\delta u$ in the formulas (4.4) for the period and area, and then using that $2\delta\beta_\delta = -1 - 2L(\beta_\delta)$, we get for $q \neq 0$ that

$$P_\delta = 2 \int_0^1 \left[1 - \beta_\delta^{1+q} \frac{2u}{q(1+q)} \frac{1-u^q}{1-u} \right]^{-1/2} \frac{du}{\sqrt{1-u}} \cdot \beta_\delta, \quad (5.14)$$

$$A_\delta = 2 \int_0^1 \left[1 - \beta_\delta^{1+q} \frac{2u}{q(1+q)} \frac{1-u^q}{1-u} \right]^{-1/2} \frac{u du}{\sqrt{1-u}} \cdot \beta_\delta^2. \quad (5.15)$$

If $q = 0$ then the same formulas hold, except with $(1 - u^q)/q$ replaced by $\log(1/u)$.

We see from (5.14) and (5.15) that P_δ and A_δ approach 0 as $\delta \rightarrow -\infty$ (i.e., as $\beta_\delta \rightarrow 0$), for all $q > -1$. These formulas also show P_δ and A_δ are strictly increasing, and approach ∞ as $\delta \rightarrow \delta(q)$.

□

Proof Proof of Result (iii), Evidence for Result (iv).

Using (5.14) and (5.15) yields $E_\delta = P_\delta^{3-q} A_\delta^{q-1} \rightarrow 0$ as $\delta \rightarrow -\infty$.

Next, since $\ell_\delta \leq \beta_\delta$ and ℓ_δ is concave (see §4), we see that the mean value A_δ/P_δ lies between $\beta_\delta/2$ and β_δ . Hence $E_\delta \rightarrow \infty$ as $\delta \rightarrow \delta(q)$, for each $q > -1$:

$$E_\delta = P_\delta^2 \left(\frac{A_\delta}{P_\delta} \right)^{q-1} \geq P_\delta^2 \beta_\delta^{q-1} \min\{1, 2^{1-q}\} \rightarrow \infty$$

because $P_\delta \rightarrow \infty$ and β_δ converges to the positive number $\beta_{\delta(q)}$.

We have proven β_δ, P_δ and A_δ are strictly increasing, and we want to do the same for E_δ . Take $\delta_1 < \delta_2 < \delta(q)$. Notice from (4.5) that if δ increases then $x(\ell)$ decreases. Hence $\ell_{\delta_1}(x) < \ell_{\delta_2}(x)$ for $0 < x \leq P_{\delta_1}/2$. This argument shows the mean value A_δ/P_δ is strictly increasing in δ , since the mean value of ℓ_{δ_1} is less than that of ℓ_{δ_2} for $0 < x < P_{\delta_1}/2$, which is less than the mean value of ℓ_{δ_2} for $0 < x < P_{\delta_2}/2$, which equals its mean value over its whole support. Therefore E_δ is strictly increasing in δ when $q \geq 1$, since $E_\delta = P_\delta^2 (A_\delta/P_\delta)^{q-1}$.

Numerical work in §6.3 suggests E_δ is strictly increasing in δ even when $-1 < q < 1$. \square

Proof Proof of Claims 5.3.1–5.3.3.

For 5.3.1, suppose we are given positive numbers P and S . Substitute $P_h = P$ and $S_h = S$ into the first of the rescaling relations in (5.11), to determine the value of P_δ . By Result (i) above, P_δ increases strictly from 0 to ∞ (as a function of δ), and so a unique value of δ exists for which P_δ attains the desired value. Now invert the rescaling (4.1) to express h in terms of ℓ_δ . By construction, h has length P and touchdown slope S , as desired, and it is the unique steady state with this property.

For 5.3.2, use Result (ii) about A_δ to argue similarly, now using the second of the rescaling relations in (5.11) instead of the first.

Finally, for 5.3.3, suppose we are given positive numbers P and A . Substitute $P_h = P$ and $A_h = A$ into (5.12), determining the value of $E_\delta = P_\delta^{3-q} A_\delta^{q-1}$. From Result (iii), E_δ ranges from 0 to ∞ (as a function of δ), and so some value of δ exists for which E_δ attains the desired value. This then determines S_h , by substituting $P_h = P, A_h = A$ into (5.11). Using this value of $S = S_h$, we invert the rescaling (4.1) to express h in terms of ℓ_δ . By construction, h has length P and area A , as desired. If $q \geq 1$ then h is the unique steady state with this property, in view of the strict monotonicity of E_δ . Since our numerical work indicates E_δ is strictly monotonic for $-1 < q < 1$, we believe h is unique when $-1 < q < 1$, as well. \square

6 The power law case — numerical computations

In this section we present numerical work on the steady states and the monotonicity properties of their length and area. We first consider the long-wave unstable equation, presenting numerical simulations of the positive periodic steady states and the touchdown steady states with zero contact angle (§6.1) and of the touchdown steady states with nonzero contact angle (§6.2). In §6.3, we present numerical results on the steady states of the long-wave stable equation.

6.1 The long-wave unstable equation — computations of positive periodic steady states and touchdown steady states with zero contact angle

Here, we discuss computations of solutions k_α of

$$k_{xx} + \frac{k^q - 1}{q} = 0, \quad k(0) = \alpha, \quad k_x(0) = 0, \quad \text{if } q \neq 0,$$

and

$$k_{xx} + \log k = 0, \quad k(0) = \alpha, \quad k_x(0) = 0, \quad \text{if } q = 0.$$

We consider a range of exponents $q > -1$ and minimum heights $\alpha \in [0, 1]$.

Given a fixed exponent q and minimum height α , we view the problem as an initial value problem, with x as the time variable. We use a fourth-order Runge–Kutta scheme to do the time-stepping. We first choose the size of the time-step by performing a convergence study for a particular pair α_0 and q_0 . We choose the time-step Δx so that the error between a computation with time-step Δx and one with time-step $\Delta x/2$ is on the order of round-off error. Since the problem becomes more regular for larger values of α and q , we use this time-step for $\alpha > \alpha_0$ and $q > q_0$.

Once the time-step Δx has been chosen, we compute the solution until its slope changes sign. We take two more time-steps to find six values: $k_x(n-3), k_x(n-2), k_x(n-1), k_x(n), k_x(n+1), k_x(n+2)$. Fitting these values with a quintic polynomial, we perform a Newton–Raphson iteration to locate the time between $(n-1)\Delta x$ and $n\Delta x$ at which the interpolating polynomial is zero. This determines the half-period $P_\alpha/2$.

Once the half-period is known, we use it to choose a smaller time-step so that re-computing the solution with this new time-step, the half-period occurs at a mesh-point. Reflecting about this mesh-point yields the solution on an entire period.

We choose the time-step so the solution is defined on $2^N = 16,384$ mesh-points. Taking the discrete Fourier transform of the culled solution yields 2^{N-1} Fourier amplitudes which, for a double precision simulation, we plot as $(k, \log(|\hat{f}(k)| + 10^{-16}))$. We consider the solution satisfactory if it is numerically indistinguishable from an analytic solution: 1) the active part of the power spectrum stays well away from the Nyquist frequency (the $N/2$ -th mode), thus ensuring that aliasing error has little effect, and 2) the remaining part of the power spectrum has amplitudes at the level of round-off error, around 10^{-14} .

In the following figures, we graph illustrative steady states for three exponents q . For each exponent q , we present seven steady states. For all the values of q , the smaller the minimum value α , the more Fourier modes are in the active part of the spectrum. This is essentially a result of the solution not being analytic when $\alpha = 0$ (see §3). We present only one set of spectra, those of the $q = -2$ solutions. The other spectra are similar.

In each figure, the steady states have the same set of seven minimum heights:

$$\alpha \in \{.0500, .2083, .3667, .5250, .6833, .8417, 1.000\}.$$

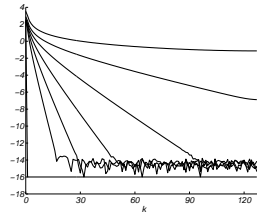
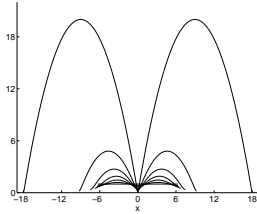


FIGURE 7. Steady states $k_\alpha(x)$, for $q = -2$.

FIGURE 8. $q = -2$ spectra.

Figure 7 shows the $q = -2$ steady states. The solution is shown over two periods to emphasize the large second derivative at $x = 0$. Both the period and the area appear to be decreasing functions of α . Figure 8 shows the spectra of the steady states; the smaller the initial height α , the more Fourier modes are active. In Figure 8 we show only the first 128 modes, but even on this scale, five of the seven solutions are numerically indistinguishable

from an analytic function. (The remaining two solutions are also indistinguishable, but need up to 5,000 of the 8,192 available modes.) Figure 9 shows $q = -1/2$ steady states,

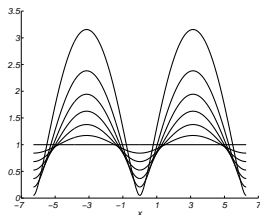


FIGURE 9. Steady states $k_\alpha(x)$, $q = -1/2$.

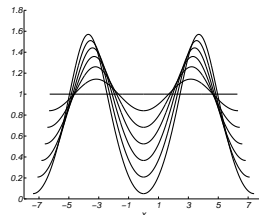


FIGURE 10. Steady states $k_\alpha(x)$, $q = 3$.

again over two periods. The period appears to be constant: in fact we proved in §3.1.3 that the period equals 2π , for all α . This allows us to use the computed period as a test of the numerical accuracy of the solutions. Doing so, we find the maximum error between the computed period and the true period is 4.1×10^{-13} .

Figure 10 shows the $q = 3$ steady states, for which the period appears to be a decreasing function of α and the area appears to be increasing.

We now consider the period P_α , the area A_α , and the invariant $E_\alpha = P_\alpha^{3-q} A_\alpha^{q-1}$ as functions of α . We find numerically that for many exponents q , the invariant E_α is either strictly decreasing or strictly increasing with α . We consider exponents $-4 \leq q \leq 10$ and minimum heights $0.005 \leq \alpha \leq 1$. For this range we find that (as functions of α)

$$\begin{array}{lll} \text{period:} & \text{decr. for } q \in [-4, -0.5), & \text{incr. for } q \in (-0.5, 1), & \text{decr. for } q \in (1, 10], \\ \text{area:} & \text{decr. for } q \in [-4, 1), & \text{incr. for } q \in (1, 5.5], & \\ \text{E:} & \text{incr. for } q \in [-4, 1), & \text{decr. for } q \in (1, 1.750], & \text{incr. for } q \in [1.750, 10]. \end{array}$$

The area is not monotonic for $5.51 \leq q \leq 10$ and E is not monotonic for $1.751 \leq q \leq 1.794$. As shown in Figure 11, E_α changes from increasing to decreasing at $q = 1$. Figure 12 shows E_α for values of $q \sim 1.77$. The value E_0 at $\alpha = 0$ was calculated from the analytic formula (3.13). In §7.2 we prove some of these numerical observations.

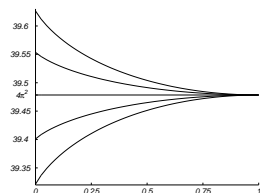


FIGURE 11. Plots of E_α for $q = .98, .99, 1.00, 1.01, 1.02$.
Bottom curve: $q = .98$.

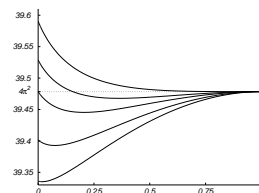


FIGURE 12. Plots of E_α for $q = 1.75, 1.76, 1.768, 1.78, 1.79$.
Top curve: $q = 1.75$.

As explained in §5.1, the loss of monotonicity shown in Figure 12 represents cases where the steady state h is not uniquely determined by its period and area. Figure 2 shows two steady states for the case $q = 1.77$, $\mathcal{B} = 40$, with equal period 1 and equal area 0.982133. These were found as follows. First we computed k_α with minimum height $\alpha_1 = 0.0519038$. Putting $P_h = 1$, $P_k = P_{\alpha_1}$ into the first scaling relation in (5.1) determined D . Then k_{α_1} yielded the first steady state h_1 by the rescaling (3.3). Proceeding similarly with $\alpha_2 = 0.386580$ gave h_2 . The minimum heights were chosen to satisfy $E(\alpha_1) = E(\alpha_2) = 39.4486$.

When two steady states are possible with the same period and area, is one of them linearly unstable and the other linearly stable? Can they both be linearly stable? Can one find two initial data h_0 and \tilde{h}_0 that have the same area and period but which converge to different steady states h_1 and h_2 as $t \rightarrow \infty$? We will consider such questions of linear and nonlinear stability in a later article.

6.2 The long-wave unstable equation — computations of touchdown steady states with nonzero contact angle

We now discuss computations of the steady states constructed in §3.2: the touchdown steady states with nonzero contact angle for the long-wave unstable equation. These solutions satisfy

$$\begin{aligned} \ell_{xx} + \frac{\ell^q}{q} - \delta &= 0, & \ell(0) &= 0, & \ell_x(0) &= 1, & \text{if } q \neq 0, \\ \text{and} \\ \ell_{xx} + \log \ell - \delta &= 0, & \ell(0) &= 0, & \ell_x(0) &= 1, & \text{if } q = 0. \end{aligned}$$

If $q \geq 0$ then the parameter $\delta \in \mathbf{R}$; if $-1 < q < 0$ then $\delta < 0$. Each δ yields a solution ℓ_δ .

It is convenient to change the initial data for computing ℓ_δ numerically, because for the above initial data the first time-step would require ℓ^q/q at $\ell = 0$, which is infinite when $q < 0$. Instead, we use as initial data: $\ell(0) = \beta_\delta$, $\ell_x(0) = 0$. That is, we translate the solution to the left and place its maximum at $x = 0$. Note that β_δ is the unique solution of $1 - 2L(y) + 2\delta y = 0$ (see §3.2) and is found using a Newton–Raphson iteration.

This choice of initial data does not cure the singular nature of the ODE at $\ell = 0$, for $-1 < q \leq 0$, and so we computed $\ell(x)$ with an adaptive time-stepping routine based on the Runge–Kutta–Fehlberg method. We stepped until h reached a value less than 10^{-15} . This yielded solutions on a non-uniform mesh, so we did not use their spectra to examine the accuracy, as we did in §6.1. Rather, we computed the solutions for the $q = 1$ case and chose the error-parameters of the adaptive scheme so that the solution and its length and area agreed up to 10^{-15} with the exact values from §3.2.1.

The ODE for ℓ_δ shows that ℓ_δ is concave if $q > 0$ and $\delta \leq 0$. For all other q and δ , the solutions are convex near the contact line. Figure 13 shows steady states for $q = 2$ and $-6 \leq \delta \leq 0$. The length of the solution increases with δ , as does the maximum height. Figure 14 shows more steady states for $q = 2$, this time with $0 \leq \delta \leq 6$. The maximum height increases as δ increases. A detailed numerical study shows the length of the solution increases till about $\delta = 0.544$ and then begins to decrease.

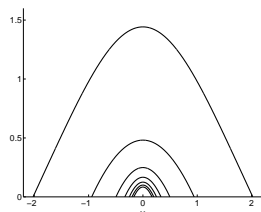


FIGURE 13. Steady states $\ell_\delta(x)$ for $q = 2$ and $\delta = -6, -5, \dots, 0$. Height increases with δ .

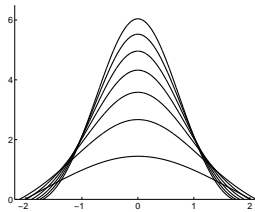


FIGURE 14. Steady states $\ell_\delta(x)$ for $q = 2$ and $\delta = 0, 1, \dots, 6$. Height increases with δ .

For exponents $-1 < q < 0$, there are solutions only for $\delta < 0$. Figure 15 shows solutions for exponent $q = -1/2$. Viewed on the scale of the height and length, these solutions look concave: the convexity near the contact line becomes apparent only on a much smaller scale.

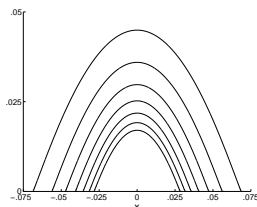


FIGURE 15. Steady states $l_\delta(x)$ for $q = -1/2$ and $\delta = -60, -55, \dots, -30$. Height increases with δ .

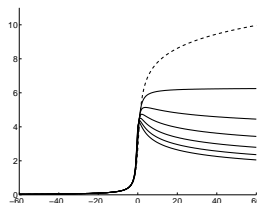


FIGURE 16. Length P_δ as a function of δ , for $q = .8, 1.0, \dots, 2.0$. Dashed line: $q = .8$.

In §5.2 we proved the length P_δ of the solution is strictly increasing when $-1 < q \leq 1$, that the area A_δ is strictly increasing when $-1 < q \leq 3$, that E_δ is strictly increasing when $1 \leq q \leq 3$, and that $\lim_{\delta \rightarrow \infty} E_\delta = E_{\alpha=0}$ for all q . We now use numerics to study these quantities for other exponents, as promised in Results (i)-(ii) of §5.2.

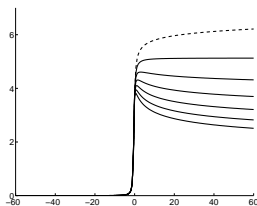


FIGURE 17. Area A_δ as a function of δ , for $q = 2.8, 3.0, \dots, 4.0$. Dashed line: $q = 2.8$.

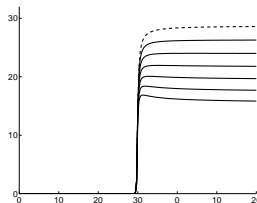


FIGURE 18. E_δ as a function of δ , for $q = 2.8, 3.0, \dots, 4.0$. Dashed line: $q = 2.8$.

Figure 16 shows the length as a function of δ , for a range of exponents near $q = 1$. The dashed curve corresponds to $q = 0.8$, and as q increases, the curves move down. The loss of monotonicity of the length for $q > 1$ is apparent, though it is not clear from the graphs that $P_\delta \rightarrow 0$ as $\delta \rightarrow \infty$, when $q > 1$, which we proved in Result (i) of §5.2. Figure 16 also indicates that when $q > 1$, P_δ increases strictly to a maximum point and then decreases strictly, as claimed in Result (i) of §5.2. Figure 17 shows the area as a function of δ for a range of exponents near $q = 3$, and Figure 18 shows the analogous plots of E_δ . In both figures, the dashed curve corresponds to $q = 2.8$, and as q increases the curves move down. For $q > 3$, we claimed in Results (ii) and (iii) of §5.2 that both the area and E increase strictly to a maximum point and then decrease strictly, as functions of δ . This is reasonably apparent even on the small range of δ -values shown in Figures 17 and 18, and when we considered the larger range $-60 \leq \delta \leq 500$, we found that

- length: increases to a maximum then decreases, when $q \in [1.00187, 10]$,
- area: increases to a maximum then decreases, when $q \in [3.00034, 10]$,
- E: increases to a maximum then decreases, when $q \in [3.02859, 10]$.

We would expect the same behavior to hold even closer to the exponents $q = 1$ and $q = 3$

if one considered even larger ranges of δ . For later reference, we denote the δ -values at which the above maxima occur by $\delta_P(q)$, $\delta_A(q)$, $\delta_E(q)$ respectively.

To address questions of non-uniqueness, we take $q = 4$ and $\mathcal{B} = 1$. Since P_δ is a non-monotonic function of δ , from Claim 5.2.1 we know how to construct two steady states h_1 and h_2 with the same length and contact angle. Such a pair of steady states is shown to the left in Figure 19, arising from $\delta_1 = -1.6$ and $\delta_2 = 31.6177$ (length = 1.24924, contact angle = 45°). Similarly, since A_δ is non-monotonic for $q = 4$, there can be two steady states with the same area and contact angle, as in the center of Figure 19: these steady states arise from $\delta_1 = -0.34$ and $\delta_2 = 17.9080$ (area = 2.90797, contact angle = 45°). Finally, E_δ is non-monotonic and so two steady states can exist with the same length and area, as in the right of Figure 19, arising from $\delta_1 = 0.64$ and $\delta_2 = 35.4592$ (length = 1, area = 2.51929).

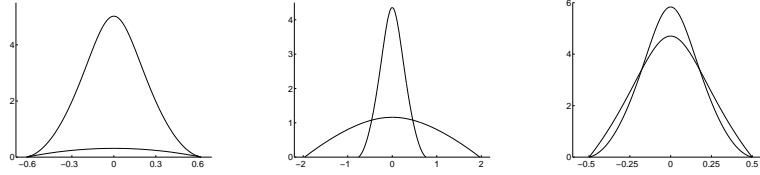


FIGURE 19. Equal: length and contact angle, area and contact angle, length and area.

In the first two cases one of the steady-state solutions is concave and the other is not, since $\delta_1 < 0 < \delta_2$. Must this always be so? To answer this question for steady states that have equal lengths and contact angles, when $q > 1$, first recall that the solutions are concave precisely when $\delta \leq 0$ and that $\delta_P(q)$ is the δ -value at which the monotonicity of P_δ changes. If $\delta_P(q) = 0$ then a horizontal line crossing the graph of P_δ will cross at two values: $\delta_1 < 0 < \delta_2$. One of the two resulting steady states will be concave, the other not. If $\delta_P(q) > 0$ then we can obtain either two non-concave steady states or else one concave and one non-concave. Similarly, if $\delta_P(q) < 0$ then we can obtain either two concave steady states or one concave and one non-concave.

For $q > 3$, the sign of $\delta_A(q)$ is similarly important for understanding steady states with equal area and contact angle. For equal length and area, $\delta_E(q)$ is what matters — but beware that $E_\delta \rightarrow E_{\alpha=0} > 0$ as $\delta \rightarrow \infty$ and so there is a lower bound on δ_1 ; for some q this lower bound is positive, which means h_1 is automatically non-concave.

Numerically, $\delta_P(q)$, $\delta_A(q)$ and $\delta_E(q)$ all seem to be strictly decreasing, with

$$\begin{aligned} \text{length:} \quad & \delta_P(q) > 0 \text{ for } q \in (1, 3), & \delta_P(q) < 0 \text{ for } q \in (3, 10], \\ \text{area:} \quad & \delta_A(q) > 0 \text{ for } q \in (3, 5), & \delta_A(q) < 0 \text{ for } q \in (5, 10], \\ \text{E:} \quad & \delta_E(q) > 0 \text{ for } q \in (3, 7.1], & \delta_E(q) < 0 \text{ for } q \in [7.2, 10], \end{aligned}$$

and with $\delta_P(3) = 0$, $\delta_A(5) = 0$, and $\delta_E(q) = 0$ for some $q \in (7.1, 7.2)$.

Next we ask whether two steady-state solutions can exist with the same length and area and with one solution having nonzero contact angle and the other having zero contact angle. For this, we rescale an ℓ_δ -solution to find h_1 and rescale a k_0 -solution to find h_2 . We need δ to satisfy

$$P_\delta^{3-q} A_\delta^{q-1} = E_\delta = E_{\alpha=0} = \frac{2}{q} (1+q) B\left(\frac{1}{2q}, \frac{1}{2}\right)^{3-q} B\left(\frac{3}{2q}, \frac{1}{2}\right)^{q-1} \quad (6.1)$$

when $q > 0$, by (3.13), with analogous formulas applying for $-1 < q \leq 0$. Our analytical and numerical evidence suggests this cannot happen when $-1 < q \leq 3$: E_δ increases to its limiting value $E_{\alpha=0}$ and so (6.1) cannot occur. When $q > 3$ there seems to be one such δ : E_δ seems to increase from 0 to its maximum and then decreases towards $E_{\alpha=0}$ (without reaching it), as in Figure 18.

Finally, we address Result (iii) of §5.2 for exponents $q \in (-1, 1)$. We examined $-0.99 \leq q \leq -0.05$ with $-50 \leq \delta \leq -5$ and $0 \leq q \leq 1$ with $-60 \leq \delta \leq 60$, and in all cases found E_δ to be strictly increasing, as claimed.

6.3 The long-wave stable equation — computations of touchdown steady states with nonzero contact angle

In this subsection, we discuss computations of the steady states constructed in §4: the touchdown steady states with nonzero contact angle of the long-wave stable equation. Translating their maxima to $x = 0$, these solutions satisfy

$$\ell_{xx} - \frac{\ell^q}{q} - \delta = 0, \quad \ell(0) = \beta_\delta, \quad \ell_x(0) = 0, \quad \text{if } q \neq 0,$$

and

$$\ell_{xx} - \log(\ell) - \delta = 0, \quad \ell(0) = \beta_\delta, \quad \ell_x(0) = 0, \quad \text{if } q = 0.$$

The maximum height β_δ is found by using a Newton–Raphson iteration to solve $1 + 2L(y) + 2\delta y = 0$. This equation has solutions for $\delta < \delta(q)$ (see §4).

We use the adaptive time-stepping scheme described in §6.2 to numerically solve the equation. We found that for the $q = 1$ case, the solution and its length and area agreed up to 10^{-15} with the exact values from §4.

From §4, the solutions are fairly well understood analytically. Specifically, they are concave for all exponents $q > -1$ and $\delta < \delta(q)$. If one fixes an exponent q and plots steady states for a range of $\delta < \delta(q)$, the resulting figure looks somewhat like Figure 13. Furthermore, §5.3 shows the length and area are increasing functions of δ , and E_δ is increasing when $q \geq 1$.

The only question remaining is whether or not E_δ is strictly increasing for exponents $-1 < q < 1$, as claimed in Result (iii) of §5.3. We considered exponents $-0.99 \leq q \leq 1$ and for each exponent took $\delta \in [\delta(q) - N - 100, \delta(q) - N]$, for some N . For $q \approx 1$, N had to be fairly close to zero before E_δ would grow noticeably. For more negative exponents q , we found N had to be quite large for the steady states to be small enough to be computable. In all cases, we found E_δ to be increasing. In Figure 20, we plot $E_{\delta(q)-N+\sigma}$ for $\sigma \in [-100, 0]$, for $q = -1/2, 0, 1/2, 1$. In each case, E_δ grows monotonically.

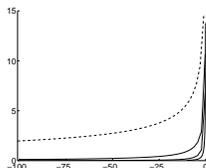


FIGURE 20. $E_{\delta(q)-N+\sigma}$ as a function of σ , for $q = -1/2, 0, 1/2, 1$. Dashed: $q = -1/2$.

7 Monotonicity of periods and areas for the positive periodic steady states

In this section, we use Theorem 7.1 to study the monotonicity of P_α , A_α , and E_α . Note below that when we claim one of these quantities is strictly increasing (decreasing) for $\alpha \in (0, 1]$, we prove it by showing slightly more, namely that the derivative is positive (negative) for $\alpha \in (0, 1)$.

We return to the positive periodic steady states k_α of the long-wave unstable equation. As we discussed in §5.1, if the invariant $E_\alpha = P_\alpha^{3-q} A_\alpha^{q-1}$ is a strictly monotonic function of α , then if there is a positive periodic steady state h with period P and volume A , it is unique.

In this section, we study the monotonicity of the invariant E_α analytically, by understanding the monotonicity properties of the period P_α and area A_α . In §7.1, we develop Theorem 7.1, a monotonicity result for the period of the nonlinear oscillator. Its proof is somewhat technical and we encourage readers to return to it after reading §7.2. In §7.2, we apply Theorem 7.1 to P_α , A_α , and E_α , proving they are monotonic in α for certain ranges of the exponent q .

7.1 An extension of a monotonicity result of Schaaf

We first recall a monotonicity result of Schaaf [43, 44] for the Hamiltonian system

$$\frac{dx}{dt} = -\mathcal{G}(y), \quad (7.1)$$

$$\frac{dy}{dt} = \mathcal{F}(x). \quad (7.2)$$

Schaaf presents two sets of conditions and proves that if the first set is satisfied then the period of the solution $(x(t), y(t))$ is an increasing function of the initial condition $x(0)$, and if the second set is satisfied then the period is decreasing:

Theorem (Schaaf [43]) *Let \mathcal{F} and \mathcal{G} be C^3 on an open interval J containing 0, with \mathcal{F} and \mathcal{G} vanishing at 0 and nowhere else, and with $\mathcal{F}'(0) > 0, \mathcal{G}'(0) > 0$. Assume either that $h = \mathcal{F}$ and $h = \mathcal{G}$ both satisfy conditions **SA(ii)** and **SA(iii)**, or that they both satisfy condition **SB(ii)**:*

$$\begin{aligned} \mathbf{SA(ii)} \quad h'(x) > 0, \quad x \in J &\implies 5h''(x)^2 - 3h'(x)h'''(x) > 0; \\ \mathbf{SA(iii)} \quad h'(x) = 0, \quad x \in J &\implies h(x)h''(x) < 0; \\ \mathbf{SB(ii)} \quad h'(x) \geq 0, \quad x \in J &\implies 5h''(x)^2 - 3h'(x)h'''(x) < 0. \end{aligned}$$

Then there is a maximal interval $(0, \alpha^+) \subset J$, $\alpha^+ > 0$, such that any solution $(x(t), y(t))$ with initial data $x(0) = \alpha \in (0, \alpha^+)$ and $y(0) = 0$ is periodic with its orbit enclosing the fixed point $(0, 0)$. Let $P(\alpha)$ be the least period of this solution. Then P is differentiable on $(0, \alpha^+)$, and for all $\alpha \in (0, \alpha^+)$,

$$\begin{aligned} P'(\alpha) > 0 &\quad \text{if } \mathcal{F} \text{ and } \mathcal{G} \text{ satisfy } \mathbf{SA(ii)} \text{ and } \mathbf{SA(iii)}, \\ P'(\alpha) < 0 &\quad \text{if } \mathcal{F} \text{ and } \mathcal{G} \text{ satisfy } \mathbf{SB(ii)}. \end{aligned}$$

For some related work on the monotonicity of periods of planar Hamiltonian systems see the papers by Chicone [18] and Rothe [42] and the book of Schaaf [44]. While Rothe's work is more general than Schaaf's, we found that for our problem it was better to extend Schaaf's results. We discuss this in detail after Proposition 7.2.

For simplicity we consider a special case, the differential equation $\ddot{x} + \mu(x) = 0$. This equation can be written as a system (7.1–7.2) with $\mathcal{F}(x) = \mu(x)$ and $\mathcal{G}(y) = y$. Although \mathcal{G} does not satisfy condition **SA(ii)** or **SB(ii)**, Schaaf [43, p. 102] noted that in this special case, her proof remains valid as long as $\mathcal{F} = \mu$ satisfies the hypotheses.

We prove an extension of Schaaf's theorem for functions μ that are C^3 on $(0, \infty)$, negative on $(0, 1)$ and positive on $(1, \infty)$, with $\mu'(1) > 0$. The fixed point of the system (7.1–7.2) is then $(1, 0)$. We consider such a system because the steady states k_α constructed in §3.1 satisfy $k'' + \mu(k) = 0$ for a particular choice of μ .

Now define M to be an antiderivative of μ ,

$$M(x) = \int_1^x \mu(s) ds,$$

chosen with $M(1) = 0$. Then M is C^4 on $(0, \infty)$ and $M(x) > 0$ for all $x \neq 1$. We use M and μ to define:

$$\nu = \frac{\mu^2 - 2M\mu'}{\mu^3} \quad \text{with} \quad \nu(1) = -\frac{\mu''(1)}{3\mu'(1)^2}. \quad (7.3)$$

The function ν is C^1 on $(0, \infty)$ and figures prominently in the proof of our theorem.

Theorem 7.1 *Assume μ is a C^3 function on $(0, \infty)$ and that μ vanishes at only one point, $\mu(1) = 0$, with $\mu'(1) > 0$. Suppose that for each $\alpha \in (0, 1)$ there is a periodic solution $x(t) > 0$ of the equation*

$$\ddot{x} + \mu(x) = 0$$

with initial data $x(0) = \alpha, \dot{x}(0) = 0$. Denote this solution by x_α and its period by $P(\alpha)$.

Let $\alpha_{min} \in [0, 1)$ and define

$$J = \cup_{\alpha \in (\alpha_{min}, 1)} \text{Range}(x_\alpha).$$

*Then J is an open interval, $J = (\alpha_{min}, \beta_{max})$ where $\beta_{max} \in (1, \infty]$. Assume that μ satisfies either the assumptions **A(ii)** and **A(iii)** or **B(ii)** and **B(iii)**:*

$$\mathbf{A(ii)} \quad \mu'(x) > 0, \quad x \in J \quad \implies \quad 5\mu''(x)^2 - 3\mu'(x)\mu'''(x) > 0.$$

$$\mathbf{A(iii)} \quad \mu'(x) = 0, \quad x \in J \quad \implies \quad \mu(x)\mu''(x) < 0.$$

B(ii) *Assume $\bar{x}_0 \in (1, \beta_{max}]$ is such that*

$$\alpha_{min} < x < \bar{x}_0 \quad \implies \quad 5\mu''(x)^2 - 3\mu'(x)\mu'''(x) < 0,$$

$$\bar{x}_0 < x < \beta_{max} \quad \implies \quad 5\mu''(x)^2 - 3\mu'(x)\mu'''(x) > 0.$$

If $\bar{x}_0 < \beta_{max}$, assume $\nu(\beta_{max}) \leq \nu(\hat{x})$ for some $\hat{x} \in (0, 1]$ with $M(\hat{x}) \leq M(\bar{x}_0)$.

$$\mathbf{B(iii)} \quad \bar{x}_0 < x < \beta_{max} \quad \implies \quad \mu'(x) > 0.$$

*Then P is a differentiable function of the initial data α . If μ satisfies **A(ii)** and **A(iii)** then $P' < 0$ on $(\alpha_{min}, 1)$. If μ satisfies **B(ii)** and **B(iii)** then $P' > 0$ on $(\alpha_{min}, 1)$.*

To maintain consistency with Schaaf's notation, there are no conditions **A(i)**, **B(i)**. In **B(ii)**, if $\beta_{max} = \infty$ then by $\nu(\beta_{max})$ we mean $\lim_{x \rightarrow \infty} \nu(x)$; we prove this limit exists.

The proof of the **A(ii)**, **A(iii)** case is a trivial modification of Schaaf's proof [43]. Our extension is the **B(ii)** case, where we allow for the possibility of $5\mu''^2 - 3\mu'\mu'''$ changing sign. Schaaf assumed this quantity was strictly negative on J .

Schaaf's periodic solutions cycle around $(0, 0)$, with initial data $(\alpha, 0)$ to the right of $(0, 0)$. Our periodic solutions cycle around $(1, 0)$, with initial data $(\alpha, 0)$ to the left of $(1, 0)$. For this reason, our monotonicity has the opposite sign to Schaaf's; her **SA(ii)** and **SA(iii)** led to $P' > 0$, while our **A(ii)** and **A(iii)** lead to $P' < 0$.

Proof Proof of Theorem 7.1

Define the Hamiltonian

$$\mathcal{E}(x, y) = M(x) + y^2/2, \quad \text{so that} \quad \frac{d}{dt} \mathcal{E}(x(t), y(t)) = 0$$

since $\dot{x} = -y, \dot{y} = \mu(x)$. We use the Hamiltonian to introduce a change of coordinates:

$$X(x) = \begin{cases} -\sqrt{M(x)} & \text{for } 0 < x \leq 1, \\ \sqrt{M(x)} & \text{for } x \geq 1, \end{cases} \quad Y(y) = \frac{y}{\sqrt{2}} \quad \text{for } y \in \mathbf{R}.$$

Then X and Y are C^2 , with $Y' > 0$ and $X' > 0$:

$$X'(x) = \frac{\mu(x)}{2X(x)} \quad \text{when } x \neq 1, \quad X'(1) = \sqrt{\frac{\mu'(1)}{2}}.$$

Let (R, Θ) be polar coordinates in the (X, Y) plane,

$$X = R \cos \Theta, \quad Y = R \sin \Theta.$$

Since X and Y are functions of x and y , so is R :

$$R = \sqrt{X^2 + Y^2} = \sqrt{M(x) + y^2/2} = \sqrt{\mathcal{E}(x, y)}.$$

By construction,

$$\frac{d}{dt} R(x(t), y(t)) = 0,$$

and the orbit $(X(x(t)), Y(y(t)))$ lies on a circle of radius $R(\alpha) \equiv R(x(0), y(0)) = -X(\alpha)$. The solution at time t is then determined by the angle, $\Theta(t)$. We now show $\Theta'(t) > 0$, so that the circle is traversed counterclockwise:

$$\Theta'(t) = \frac{d}{dt} \arctan \frac{Y(y(t))}{X(x(t))} = \frac{X(x)Y'(y)\dot{y}(t) - Y(y)X'(x)\dot{x}(t)}{X(x)^2 + Y(y)^2} = \sqrt{2}X'(x(t)) > 0.$$

Hence $\Theta(t)$ is C^2 , since $X \in C^2$. As $x(t)$ goes through one period, $\Theta(t)$ increases by 2π .

Thus, for fixed α , the range of $X(x(t))$ is $[-R(\alpha), R(\alpha)]$ and the range of $x(t)$ is $[X^{-1}(-R(\alpha)), X^{-1}(R(\alpha))]$. Because $R(\alpha) = -X(\alpha)$ it follows that J is the open interval

$$J = \cup_{\alpha \in (\alpha_{min}, 1)} [\alpha, X^{-1}(-X(\alpha))] = (\alpha_{min}, X^{-1}(-X(\alpha_{min}))) = (\alpha_{min}, \beta_{max}).$$

From above, $\Theta(t)$ is an invertible function of t and

$$t'(\Theta) = \frac{1}{\Theta'(t)} = \frac{1}{\sqrt{2}X'(x(t(\Theta)))}.$$

We simplify this by noting that $X(x(t)) = R \cos \Theta(t) \implies x(t(\Theta)) = X^{-1}(R \cos \Theta)$. Hence

$$t'(\Theta) = \frac{1}{\sqrt{2}}(X^{-1})'(R \cos \Theta).$$

Observe that $t'(\Theta)$ depends on α through the α -dependence of $R = -X(\alpha)$.

We now compute the period of the solution x_α :

$$P(\alpha) = \int_{-\pi}^{\pi} t'(\Theta) d\Theta = \frac{1}{\sqrt{2}} \int_{-\pi}^{\pi} (X^{-1})'(R \cos \Theta) d\Theta.$$

Since X^{-1} is C^2 , we can differentiate $P(\alpha)$ through the integral, yielding

$$\begin{aligned} P'(\alpha) &= \frac{1}{\sqrt{2}} \frac{dR}{d\alpha} \int_{-\pi}^{\pi} (X^{-1})''(R \cos \Theta) \cos \Theta d\Theta \\ &= -\sqrt{2} X'(\alpha) \int_0^{\pi/2} [(X^{-1})''(R \cos \Theta) - (X^{-1})''(-R \cos \Theta)] \cos \Theta d\Theta. \end{aligned}$$

Since $X'(\alpha) > 0$, the monotonicity of $P(\alpha)$ now follows from the following claim:

Theorem 7.1 *If μ satisfies the assumptions **A(ii)** and **A(iii)** then*

$$(X^{-1})''(W) < (X^{-1})''(-W) \quad \text{for all } W \in (X(\alpha_{min}), 0).$$

*If μ satisfies the assumptions **B(ii)** and **B(iii)** then the inequality is reversed.*

Proof of Claim. We first compute

$$(X^{-1})'(W) = \frac{1}{X'(X^{-1}(W))} \quad \text{and} \quad (X^{-1})''(W) = -\frac{X''}{(X')^3}(X^{-1}(W)).$$

For $x \neq 1$,

$$X'(x) = \frac{\mu(x)}{2X(x)} \quad \text{and} \quad X''(x) = \frac{X(x)\mu'(x) - \mu(x)^2/2X(x)}{2X(x)^2},$$

and so

$$(X^{-1})''(W) = 2 \left(\frac{\mu^2 - 2X^2\mu'}{\mu^3} \right) (X^{-1}(W)) = 2\nu(X^{-1}(W)).$$

Writing $x = X^{-1}(W)$ and $\bar{x} = X^{-1}(-W) = X^{-1}(-X(x))$, we see that to prove the first part of the claim it suffices to prove that when **A(ii)** and **A(iii)** hold,

$$\nu(x) < \nu(\bar{x}) \quad \text{whenever } \alpha_{min} < x < 1.$$

For the **B(ii)** and **B(iii)** case, we prove the inequality is reversed. With this notation, $J = (\alpha_{min}, \beta_{max}) = (\alpha_{min}, \overline{\alpha_{min}})$.

We first prove the claim under the assumptions **A(ii)** and **A(iii)**. The proof is essentially identical to Schaaf's proof and is provided for the reader's convenience.

Because $\mu'(1) > 0$, there is a maximal interval $(x_1, \bar{x}_2) \subset J$, with $\alpha_{min} \leq x_1, x_2 < 1$, on which $\mu' > 0$. We first show that

$$\nu' > 0 \quad \text{on } (x_1, \bar{x}_2). \quad (7.4)$$

At $x = 1$ we have

$$\nu'(1) = \frac{1}{12\mu'(1)^3} [5\mu''(1)^2 - 3\mu'(1)\mu'''(1)] > 0, \quad (7.5)$$

by **A(ii)**, and for $x \neq 1$ we have

$$\nu'(x) = -\frac{S(x)}{\mu(x)^4}$$

where

$$S = 2M\mu\mu'' + 3\mu'(\mu^2 - 2M\mu') \quad \text{and} \quad S' = 2M\mu\mu''' + 5\mu''(\mu^2 - 2M\mu').$$

By (7.5), $S(x)$ is negative for x near 1. Suppose there is a first zero \bar{x}_0 of S with $\bar{x}_0 \in (1, \bar{x}_2)$. Then $S'(\bar{x}_0) \geq 0$. From $S(\bar{x}_0) = 0$ we deduce

$$(\mu^2 - 2M\mu')(\bar{x}_0) = -\frac{2M\mu\mu''}{3\mu'}(\bar{x}_0),$$

and thus

$$S'(\bar{x}_0) = \frac{2M\mu}{3\mu'}(\bar{x}_0) [3\mu'''\mu' - 5(\mu'')^2](\bar{x}_0) < 0,$$

by **A(ii)** and since $\mu(\bar{x}_0) > 0$. This is impossible, therefore $S < 0$ and hence $\nu' > 0$ on $(1, \bar{x}_2)$. A similar argument shows $S < 0$ and hence $\nu' > 0$ on $(x_1, 1)$, proving (7.4) holds.

If $(x_1, \bar{x}_2) = J$ then we are done, since $x < \bar{x}$ and $\nu' > 0$ on (x, \bar{x}) implies $\nu(x) < \nu(\bar{x})$. Assume $(x_1, \bar{x}_2) \neq J$, so that either $x_1 > \alpha_{min}$ or $x_2 > \alpha_{min}$. There are four possible cases:

$$\begin{aligned} \alpha_{min} < x_2 \leq x_1 < 1, & \quad \alpha_{min} < x_1 \leq x_2 < 1, \\ \alpha_{min} = x_2 < x_1 < 1, & \quad \alpha_{min} = x_1 < x_2 < 1. \end{aligned}$$

Assume the first case: $\alpha_{min} < x_2 \leq x_1 < 1$. Then $\mu'(x_1) = 0$ and $\mu'(\bar{x}_2) = 0$ by definition of x_1 and x_2 . By Condition **A(iii)**, $\mu''(x_1) > 0$ and hence $\mu' < 0$ on (α_{min}, x_1) . Similarly, $\mu''(\bar{x}_2) < 0$ and hence $\mu' < 0$ on (\bar{x}_2, β_{max}) , by **A(iii)**. It follows that

$$x \in (\alpha_{min}, x_1) \implies \nu(x) < \frac{1}{\mu(x)} \quad \text{and} \quad x \in (\alpha_{min}, x_2) \implies \frac{1}{\mu(\bar{x})} < \nu(\bar{x}).$$

We now prove that if $x \in (\alpha_{min}, 1)$ then $\nu(x) < \nu(\bar{x})$. There are three possibilities: $x \in (\alpha_{min}, x_2)$, $x \in [x_2, x_1)$, and $x \in [x_1, 1)$.

If $x \in (\alpha_{min}, x_2)$ then $\bar{x}_2 < \bar{x}$. It follows that

$$0 < \nu(\bar{x}_2) = \frac{1}{\mu(\bar{x}_2)} < \frac{1}{\mu(\bar{x})} < \nu(\bar{x}).$$

On the other hand, since $x_2 \leq x_1$,

$$\nu(x) \leq \frac{1}{\mu(x)} < 0.$$

Therefore $\nu(x) < \nu(\bar{x})$.

If $x \in [x_2, x_1)$ then $\bar{x} \leq \bar{x}_2$. Since $\nu' > 0$ on (x_1, \bar{x}_2) ,

$$\nu(x_1) < \nu(\bar{x}).$$

On the other hand, since $x < x_1$,

$$\nu(x) < \frac{1}{\mu(x)} < \frac{1}{\mu(x_1)} = \nu(x_1).$$

Combining these two inequalities, we see $\nu(x) < \nu(\bar{x})$.

Finally, if $x \in [x_1, 1)$ then $\bar{x} \leq \bar{x}_2$. Since $\nu' > 0$ on (x_1, \bar{x}_2) , it follows immediately that $\nu(x) < \nu(\bar{x})$.

The remaining three cases, $\alpha_{min} < x_1 \leq x_2 < 1$, $\alpha_{min} = x_2 < x_1 < 1$, and $\alpha_{min} = x_1 < x_2 < 1$, are argued in a similar manner.

Now replace the assumptions **A(ii)** and **A(iii)** by assumptions **B(ii)** and **B(iii)**. To prove the claim we want to prove

$$\nu(x) > \nu(\bar{x}) \quad \text{whenever} \quad \alpha_{min} < x < 1.$$

Assumption **B(ii)** implies

$$\alpha_{min} < x < \bar{x}_0 \quad \implies \quad 0 \leq 5\mu''(x)^2 < 3\mu'(x)\mu'''(x).$$

Thus $\mu' \neq 0$ on $(\alpha_{min}, \bar{x}_0)$. Because $\mu'(1) > 0$, it follows that $\mu' > 0$ on $(\alpha_{min}, \bar{x}_0)$. Since for the **B(ii)** case, $\nu'(1) < 0$ by (7.5), one can argue as before to prove the analogue of (7.4): $\nu' < 0$ on $(\alpha_{min}, \bar{x}_0)$.

Hence if $\nu' \leq 0$ on J then $\nu(\bar{x}) < \nu(x)$ whenever $\alpha_{min} < x < 1$ and we are done. Assume instead from now on that $\nu' > 0$ somewhere on J , which obviously requires $\bar{x}_0 < \beta_{max}$. Define

$$\bar{x}_3 = \inf \{x \in [\bar{x}_0, \beta_{max}) : \nu'(x) > 0\}.$$

We now prove that

$$\nu' > 0 \quad \text{on} \quad (\bar{x}_3, \beta_{max}).$$

Assume not. Then there is some $x \in (\bar{x}_3, \beta_{max})$ with $\nu'(x) > 0$, but with $\nu'(\bar{x}_4) = 0$ for some $\bar{x}_4 \in (x, \beta_{max})$. Take \bar{x}_4 to be the smallest number with this property. Since $S(\bar{x}_4) = 0$,

$$(\mu^2 - 2M\mu')(\bar{x}_4) = -\frac{2M\mu\mu''}{3\mu'}(\bar{x}_4)$$

and thus since $\mu'(\bar{x}_4) > 0$ by **B(iii)**,

$$S'(\bar{x}_4) = \frac{2M\mu}{3\mu'}(\bar{x}_4) [3\mu'''\mu' - 5(\mu'')^2](\bar{x}_4) < 0$$

by **B(ii)**. However, ν' is positive to the left of \bar{x}_4 and so S is negative there, implying $S'(\bar{x}_4) \geq 0$. This is impossible. Therefore if $x \in (\bar{x}_3, \beta_{max})$ with $\nu'(x) > 0$ then $\nu' > 0$ on (x, β_{max}) . It then follows that $\nu' > 0$ on (\bar{x}_3, β_{max}) .

To summarize, we have proved that

$$\begin{aligned} \alpha_{min} < x < \bar{x}_0 &\implies \nu'(x) < 0, \\ \bar{x}_0 \leq \bar{x} \leq \bar{x}_3 &\implies \nu'(\bar{x}) \leq 0, \\ \bar{x}_3 < \bar{x} < \beta_{max} &\implies \nu'(\bar{x}) > 0. \end{aligned}$$

The first two implications show $\nu(x) > \nu(\bar{x})$ whenever $x_3 \leq x < 1$. The third implies $\nu(\beta_{max})$ exists as a limiting value. By assumption **B(ii)**, $\nu(\beta_{max}) \leq \nu(\hat{x})$ and

$$M(\hat{x}) \leq M(\bar{x}_0) \leq M(\bar{x}_3) = M(x_3),$$

which implies $x_3 \leq \hat{x} \leq 1$ and so $\nu(\hat{x}) \leq \nu(x_3)$. Thus

$$\alpha_{min} < x < x_3 \quad \implies \quad \nu(\bar{x}) < \nu(\beta_{max}) \leq \nu(\hat{x}) \leq \nu(x_3) < \nu(x),$$

finishing the proof. □

7.2 Monotonicity of $P_\alpha, A_\alpha, E_\alpha$

In this section, we use Theorem 7.1 to study the monotonicity of $P_\alpha, A_\alpha,$ and E_α .

Theorem 7.1 *The period P_α has*

$$\frac{dP_\alpha}{d\alpha} \begin{cases} < 0 \text{ for all } \alpha \in (0, 1) & \text{if } q < -1/2 \text{ or } q > 1; \\ > 0 \text{ for all } \alpha \in (0, 1) & \text{if } -1/2 < q < 1. \end{cases}$$

For the exponents $q = -1/2$ and $q = 1$ we saw in §3.1.3 that $P \equiv 2\pi$. Furter and Eilbeck [24] obtained the Proposition for $q < 0$, and also noted the constancy of the period when $q = -1/2$. (See [24, Prop. 4.5(a)] with $q = 1/(1 - p)$.)

Theorem 7.2 *The area A_α has*

$$\frac{dA_\alpha}{d\alpha} \begin{cases} < 0 \text{ for all } \alpha \in (0, 1) & \text{if } q < 1; \\ > 0 \text{ for all } \alpha \in (0, 1) & \text{if } 1 < q \leq 4.54. \end{cases}$$

For $4.54 < q < 5.5$, A_α is strictly increasing on $[\alpha_1(q), 1]$, where $\alpha_1(q) \in (0, 1)$ is the solution of $H(\alpha_1(q)) = H(\beta_1(q))$ and

$$\beta_1(q) = \left(\frac{3(q+2)}{2(q-1)(q-3)} \right)^{1/q} \in (1, (1+q)^{1/q}).$$

For $q > 5.5$, A_α is strictly decreasing on $[\alpha_2(q), 1]$, where

$$\alpha_2(q) = \left(\frac{3(q+2)}{2(q-1)(q-3)} \right)^{1/q} \in (0, 1).$$

In §3.1.3, we proved that $A \equiv 2\pi$ for the exponent $q = 1$. Also, our numerical work suggests that the area is monotonic on $(0, 1]$ for all $q \in (1, 5.5]$, although the proposition proves this only up to $q = 4.54$. We will explain how to extend our methods to $q = 4.82$, but since this extension relies on a numerical plot of a function of one variable, it is not rigorous. Proposition 7.2 does show that the area changes monotonicity at $q = 5.5$, for a range of α near 1. The numerics for $q > 5.5$ show further that A_α is not monotonic on all of $(0, 1]$.

The hypothesis “(f4)⁻” of Rothe [42] can be shown to hold for $1 < q \leq 4.44$, hence yielding monotonicity, but it fails for $q \geq 4.45$. Rothe’s other main hypothesis, (F4)⁻,

seems difficult to verify analytically and in any case fails for $q = 4.55$ (because it is equivalent to $\gamma > 0$ in our proof, and $\gamma(4.55) < 0$). Thus our extension of Schaaf's method, in Theorem 7.1, offers more hope of progress towards $q = 5.5$.

Recalling that $E_\alpha = P_\alpha^{3-q} A_\alpha^{q-1}$, we combine Propositions 7.1 and 7.2 to obtain:

Theorem 7.2

$-1/2 \leq q < 1$ and $3 \leq q \leq 4.54$: E_α is a strictly increasing function of $\alpha \in (0, 1]$.

The numerical work we presented in §6.1 indicates E_α is strictly increasing on $(0, 1]$ when $q \in [-4, 1)$, strictly decreasing when $q \in (1, 1.750]$, and strictly increasing when $q \in [1.795, 10]$, but that E_α is not monotonic for $q \in [1.751, 1.794]$.

Proof Proof of Proposition 7.1.

Recall that we are considering $k'' + \mu(k) = 0$ where

$$\mu(y) = \begin{cases} \frac{y^q - 1}{q} & \text{if } q \neq 0, \\ \log y & \text{if } q = 0, \end{cases} \quad \text{for } y > 0.$$

The solutions $k_\alpha(x)$ were constructed in Section 3.1, where we observed $P_\alpha \rightarrow P_1 = 2\pi$ as $\alpha \rightarrow 1$.

Clearly μ is smooth, with $\mu(1) = 0$ and $\mu'(y) > 0$ for all $y \in (0, \infty)$. Take $\alpha_{min} = 0$. To check conditions **A(ii)** and **B(ii)** in Theorem 7.1, we compute

$$5\mu''(y)^2 - 3\mu'(y)\mu'''(y) = (q-1)(2q+1)y^{2q-4}.$$

Condition **A(ii)** holds for $q < -1/2$, $q > 1$. As μ' never vanishes, condition **A(iii)** holds trivially. For $-1/2 < q < 1$ take $\bar{x}_0 = \beta_{max}$. Then condition **B(ii)** is satisfied and **B(iii)** holds trivially. Now apply Theorem 7.1. \square

Proof Proof of Proposition 7.2.

We prove monotonicity for the area by applying Theorem 7.1 to a differential equation whose period equals the area A . Writing $k = k_\alpha$, define $I(x) = \int_0^x k(s) ds$. Then I is strictly increasing since $I'(x) = k(x) \geq \alpha > 0$ for all x . Define

$$k_*(y) = k(I^{-1}(y))^2 \quad \text{for } y \in \mathbf{R},$$

so that $k_*(y)$ has minimum value $\alpha_* = \alpha^2$ and maximum value $\beta_* = \beta^2$. By construction, the period of k_* equals A_α , the area under k . For $z > 0$, define

$$\mu_*(z) = \frac{2\mu(\sqrt{z})}{\sqrt{z}} = \begin{cases} 2(z^{q/2} - 1)/(q\sqrt{z}) & \text{if } q \neq 0, \\ (\log z)/\sqrt{z} & \text{if } q = 0. \end{cases}$$

Then $k_*(y)$ satisfies

$$k_*'' + \mu_*(k_*) = 0.$$

Clearly μ_* is smooth with μ_* vanishing only at $z = 1$, and $\mu_*(1) > 0$. Also, $M_*(z) = 4M(\sqrt{z})$ satisfies $M_*' = \mu_*$ since $M(y) = H(y) - H(1)$ satisfies $M' = \mu$. (The function H was defined in (3.6).)

We first consider the $q = 0$ case. In this case,

$$\mu'_*(z) = z^{-3/2}[2 - \log z]/2, \quad \mu''_*(z) = z^{-5/2}[-8 + 3 \log z]/4, \quad \mu'''_*(z) = z^{-7/2}[46 - 15 \log z]/8.$$

For condition **A(iii)**, $\mu'_*(z) = 0$ implies $z = e^2$ and so $\mu_*(z)\mu''_*(z) = -e^{-6} < 0$. For condition **A(ii)**, $\mu'_*(z) > 0 \implies \log z < 2$ and hence

$$5\mu''_*(z)^2 - 3\mu'_*(z)\mu'''_*(z) = (11 - 3 \log z)z^{-5}/4 > 5z^{-5}/4 > 0.$$

Thus condition **A(ii)** holds with $\alpha_{min} = 0$, and the area is monotonically decreasing by Theorem 7.1.

We now consider the $q \neq 0$ case. In this case,

$$\begin{aligned} \mu'_*(z) &= z^{-3/2} \left[(q-1)z^{q/2} + 1 \right] / q, \\ \mu''_*(z) &= z^{-5/2} \left[(q-1)(q-3)z^{q/2} - 3 \right] / 2q, \\ \mu'''_*(z) &= z^{-7/2} \left[(q-1)(q-3)(q-5)z^{q/2} + 15 \right] / 4q. \end{aligned}$$

Consider assumption **A(iii)**. Assume there is a point $z > 0$ at which $\mu'_*(z) = 0$. Then $(1-q)z^{q/2} = 1$ and so $q < 1$. Hence

$$\mu_*(z) = 2z^{-1/2}/(1-q) > 0, \quad \mu''_*(z) = -z^{-5/2}/2 < 0 \quad \implies \quad \mu_*(z)\mu''_*(z) < 0,$$

and **A(iii)** holds.

We now consider conditions **A(ii)** and **B(ii)**. Start by computing

$$5\mu''_*(z)^2 - 3\mu'_*(z)\mu'''_*(z) = z^{(q-10)/2} \left(\frac{q-1}{4q} \right) \left[2(q-1)(q-3)z^{q/2} - 3(q+2) \right]. \quad (7.6)$$

To establish Condition **A(ii)**, for certain q -values, we will show that expression (7.6) is positive for all z with $\mu'_*(z) > 0$. To establish Condition **B(ii)** for other q -values, we will show the quantity is negative for $z < \bar{z}_0$ and positive for $z > \bar{z}_0$, for some $\bar{z}_0 > 1$.

Condition **A(ii)**:

If $q < 0$ and $\mu'_*(z) > 0$ then $(1-q)z^{q/2} > 1$. It follows that (7.6) is greater than $5z^{(q-10)/2}(1-q)/4$, which is positive. Thus Condition **A(ii)** holds with $\alpha_{min} = 0$.

If $0 < q < 1$ and $\mu'_*(z) > 0$ then $(1-q)z^{q/2} < 1$. Again, (7.6) is bounded below by $5z^{(q-10)/2}(1-q)/4$, which is positive, and so Condition **A(ii)** holds with $\alpha_{min} = 0$.

Finally, assume $q > 5.5$. For

$$z > \alpha_2(q)^2 = \left(\frac{3(q+2)}{2(q-1)(q-3)} \right)^{2/q},$$

(7.6) is positive, and so Condition **A(ii)** holds for $\alpha_{min} = \alpha_2(q)^2$. The exponent 5.5 is critical since $\alpha_2(5.5) = 1$.

Conditions **B(ii)** and **B(iii)**:

For $q > 1$, we first observe that $\mu'_*(z) > 0$ for all z , and so **B(iii)** holds.

If $1 < q \leq 3$, then (7.6) is negative and so Condition **B(ii)** is satisfied with $\alpha_{min} = 0$, $\bar{z}_0 = \beta_{max}$.

Next define $z_{max} = (1+q)^{2/q}$. Then $1 < z_{max}$ and $k_*(y) = k(I^{-1}(y))^2 < z_{max}$ for all y and all $\alpha \in (0, 1)$.

Now assume that $3 < q \leq (\sqrt{19} + 3)/2$. For $z < z_{max} = (1+q)^{2/q}$, (7.6) gives

$$5\mu_*''(z)^2 - 3\mu_*'(z)\mu_*'''(z) < z^{(q-10)/2} \left(\frac{q-1}{2}\right) \left(q - \frac{\sqrt{19}+3}{2}\right) \left(q + \frac{\sqrt{19}-3}{2}\right) \leq 0.$$

Hence Condition **B(ii)** is satisfied, with $\alpha_{min} = 0$, $\bar{z}_0 = \beta_{max} = z_{max}$.

Now assume that $(\sqrt{19} + 3)/2 < q < 5.5$. If

$$z < \beta_1(q)^2 = \left(\frac{3(q+2)}{2(q-1)(q-3)}\right)^{2/q}$$

then (7.6) is negative and Condition **B(ii)** holds for $\alpha_{min} = \alpha_1(q)^2$, $\beta_{max} = \beta_1(q)^2$ and $\bar{z}_0 = \beta_{max}$. The value of 5.5 is critical for this upper bound since $\beta_1(5.5) = 1$.

For the smaller range $(\sqrt{19} + 3)/2 < q \leq 4.54$, we obtain a better result. If $z < \beta_1(q)^2$ then (7.6) is negative while if $z > \beta_1(q)^2$ then (7.6) is positive. Thus to establish **B(ii)** for $\alpha_{min} = 0$, $\beta_{max} = z_{max}$ and $\bar{z}_0 = \beta_1(q)^2 < \beta_{max}$, it suffices to take $\hat{z} = 1$ and prove $\nu_*(\beta_{max}) \leq \nu_*(1)$. We calculate

$$\nu_*(1) = -\frac{\mu_*''(1)}{3\mu_*'(1)^2} = \frac{4-q}{6}$$

by using (7.3). For $\beta_{max} = z_{max} = (1+q)^{2/q}$,

$$\begin{aligned} \mu_*((1+q)^{2/q}) &= 2(1+q)^{-1/q}, & \mu_*'((1+q)^{2/q}) &= q(1+q)^{-3/q}, \\ \text{and } M_*((1+q)^{2/q}) &= 4(1+q)^{-1}, \end{aligned}$$

and hence

$$\nu_*((1+q)^{2/q}) = \frac{(1+q)^{1/q}}{2} - \frac{q}{1+q}.$$

Defining

$$\gamma(q) = \nu_*(1) - \nu_*((1+q)^{2/q}) = \frac{4-q}{6} - \frac{(1+q)^{1/q}}{2} + \frac{q}{1+q},$$

it remains to prove that $\gamma(q) \geq 0$ on $((\sqrt{19} + 3)/2, 4.54]$. For $q \in ((\sqrt{19} + 3)/2, 4)$, this follows from the facts that $\nu_*(1) > 0$, $\nu_*((1+q)^{2/q}) < 0$ when $q = (\sqrt{19} + 3)/2$, and

$$\frac{d}{dq}\nu_*((1+q)^{2/q}) = \frac{(1+q)^{1/q}}{2q} \left[-\frac{1}{q}\log(1+q) + \frac{1}{1+q}\right] - \frac{1}{(1+q)^2} < -\frac{1}{(1+q)^2} < 0$$

for all $q > 0$. Also, direct computation shows that $\gamma(4.54) > 0$ and $\gamma(4.55) < 0$, and we show below that $\gamma'(q) < 0$ for $q \geq 4$; hence $\gamma(q) > 0$ for $4 \leq q \leq 4.54$. It remains to prove that $\gamma'(q) < 0$ for $q \geq 4$:

$$\begin{aligned} \gamma'(q) &= -\frac{1}{6} + \frac{(1+q)^{1/q}}{2q} \left[\frac{1}{q}\log(1+q) - \frac{1}{1+q}\right] + \frac{1}{(1+q)^2} \\ &\leq -\frac{1}{6} + \frac{(1+q)^{1/q}}{2q} \left[\frac{1}{\sqrt{q}} - \frac{1}{\sqrt{q}(1+q)}\right] + \frac{1}{(1+q)^2} \\ &= -\frac{1}{6} + \frac{1}{2\sqrt{q}(1+q)^{1-1/q}} + \frac{1}{(1+q)^2} \quad \text{which is decreasing in } q, \text{ and so} \end{aligned}$$

$$\leq -\frac{1}{6} + \frac{1}{2\sqrt{4}(1+4)^{1-1/4}} + \frac{1}{(1+4)^2} < 0.$$

Thus $\gamma > 0$ on $((\sqrt{19} + 3)/2, 4.54]$, as desired.

Hence Condition **B(ii)** holds for $(\sqrt{19} + 3)/2 < q \leq 4.54$, with $\alpha_{min} = 0, \beta_{max} = z_{max} = (1+q)^{2/q}$ and $\bar{z}_0 = \beta_1(q)^2, \hat{z} = 1$.

Collecting the above results and applying Theorem 7.1 proves the proposition. \square

We now explain how to improve the exponent in Proposition 7.2 from 4.54 to 4.82. In the last part of the proof, we would like to take $\hat{z} = \alpha_1(q)^2$ (rather than $\hat{z} = 1$), which would work because

$$M_*(\alpha_1(q)^2) = 4M(\alpha_1(q)) = 4M(\beta_1(q)) = M_*(\beta_1(q)^2) = M_*(\bar{z}_0).$$

But this choice of \hat{z} would be impractical, since we have no explicit formula for $\alpha_1(q)$. We can take $\hat{z} = [2 - \beta_1(q)]^2$, though, with $M_*(\hat{z}) < M_*(\bar{z}_0)$ since \hat{z} lies between $\alpha_1(q)^2$ and 1, as we now show. In fact, $1 - \alpha_1(q) > \beta_1(q) - 1$ by the positivity of the second and third derivatives of $M(y)$, and since $M'(1) = 0$ and $M(\alpha_1(q)) = M(\beta_1(q))$; hence $\alpha_1(q)^2 < \hat{z} < 1$. Finally, using this \hat{z} , a *Mathematica* plot clearly shows that $\nu_*(\beta_{max}) \leq \nu_*(\hat{z})$ when $q \in [4, 4.82]$, and so condition **B(ii)** holds up to $q = 4.82$.

8 Future directions

We close the article with a discussion of two natural directions in which this work leads. One is to relate the steady states to a finite-time blow-up conjecture. The other is to study the linear and nonlinear stability of the steady states, as well as to study the evolution of initial data whose period and area are such that there are no steady states having that period and area to which it could relax.

Relevance to a finite-time blow-up conjecture

In a recent article, Bertozzi and Pugh [13] made a conjecture about the possibility of finite-time blow-up in long-wave unstable equations. Here, we will relate the conjecture to the behavior of the class of steady states that rescale to a fixed k_α .

Their conjecture concerns the class of degenerate equations, $f(0) = 0$, for which $|g(y)/f(y)|$ is bounded as $y \rightarrow 0$. The conjectured blow-up is determined by the large- y behavior of the coefficients: for $f(y) \sim y^n > 0$, $g(y) \sim y^m > 0$ for $y \gg 1$, with $q = m - n + 1$, their conjecture claims that

if $q > 3$ and $m > n/2$, then for suitable initial data, $\|h(\cdot, t)\|_\infty \rightarrow \infty$ in finite time.

For $q < 3$, they prove $\|h(\cdot, t)\|_\infty$ is bounded for all time, for all initial data. For $q \geq 3$ and $m \leq n/2$, they show $\|h(\cdot, t)\|_\infty$ can grow at most exponentially. They make no conjecture for the critical case, $q = 3$ and $m > n/2$.

Bertozzi and Pugh support their conjecture with numerical simulations of a supercritical case, $q > 3$ and $m > n/2$, which shows a finite-time $h \uparrow \infty$ singularity. Their simulation of a critical case, $q = 3$ and $m > n/2$, displays three simultaneous singularities: as $t \uparrow t_0 < \infty$ there is a blow-up singularity, $h(x_0, t) \uparrow \infty$, as well as a pair of pinching singularities, $h(x_1, t) \downarrow 0$ and $h(x_2, t) \downarrow 0$, one to each side of x_0 .

Let us assume that a solution h is blowing up in finite time at a point x_0 : $h(x_0, t) \uparrow \infty$ as $t \rightarrow t_0$. Let us further assume that in a neighborhood of the singular point the solution of the evolution equation is approximated by a family of periodic steady-state solutions and that these steady-state solutions all rescale via (3.3) to the same rescaled steady state $k_\alpha(x)$. (This would correspond to a self-similar solution of the second kind, *à la* Zeldovitch. We refer the interested reader to Barenblatt [2] for many examples, including those on pinching singularities for the equation $h_t = -(h^n h_{xxx})_x$.) The solution h conserves volume as it evolves. Thus if it is locally approximated by such a family of steady states then the periods P_h of these steady states must go to zero as the singular time approaches and h blows up (since otherwise the volume A_h would go to infinity). We recall (5.2), the invariance relation

$$\mathcal{B}P_h^{3-q} A_h^{q-1} = E_\alpha, \quad \text{which implies} \quad \mathcal{B}A_h^{q-1} = E_\alpha P_h^{q-3}.$$

Thus if $q > 3$, the approximating steady states have decreasing volume as the singular time approaches (as P_h goes to zero). If $q = 3$, the approximating steady states have fixed volume as the singular time approaches. If $q < 3$ then the volume of the approximating steady states would increase to infinity, as the singular time approached, which is an impossibility. In this way, the steady states and their scaling properties are consistent with the conjecture.

Simulations by Bertozzi and Pugh [9] for the supercritical case, $q > 3$ and $m > n/2$, suggest that near the singular point the solution behaves like a self-similar solution of the first kind — that is, like a self-similar solution of the evolution equation. But their simulations of the critical case, $q = 3$ and $m > n/2$, suggest the solution is indeed behaving like a self-similar solution of the second kind. This leads us to believe that the steady-state solutions and their scaling properties may yield insight into blow-up in the critical case — currently a poorly understood phenomenon.

Stability and large-time behavior

We have established properties of the steady-state solutions of the evolution equation

$$h_t = -(f(h)h_{xxx})_x - (g(h)h_x)_x,$$

for power-law coefficients f and g . Now that we understand these steady states, a future goal is to investigate their linear and nonlinear stability and large-time behavior.

Consider an initial profile for the evolution equation (1.1), with period P and area A . In this article we found three possibilities: there can be zero, one or two positive periodic steady states with period P and area A .

If there is only one such steady state and the initial profile is a small periodic perturbation of it, will the solution relax to the steady state, or will it evolve and relax to some other steady state, or will it have non-steady long-time behavior? If the steady state is linearly stable then one would expect the solution to relax to it. On the other hand, if the steady state is linearly unstable then it has a “most unstable” mode, and since the evolution equation is nonlinear, this mode’s wavelength should become dominant in the evolution. This suggests the period of the solution might change as time passes. For example, if the second mode were the most unstable, perhaps the period would halve and the solution would relax to a steady state with period $P/2$ and area $A/2$.

If there are two steady states having the same period and area as the initial profile, then will the solution relax to one of them, and if so, which one? Or might the solution change its period and relax to a completely different steady state? Might it have non-steady large-time dynamics?

Also, it could be that certain initial profiles have area and period that render the solution unable to relax to *any* steady state — suggesting interesting large-time behavior.

We plan to investigate some of these questions in a future article.

For the touchdown steady states there are analogous questions, along with new and challenging questions about large-time behavior. For example, the computations of Bertozzi and Pugh for a subcritical case suggest that as time goes to infinity the solution relaxes to a disjoint collection of steady states each with bounded support, *i.e.*, to separated droplets. One can translate any one of these droplets and still have a steady state, as long as the droplets remain disjoint. How does the solution select to which of these infinitely many possible configurations it will relax?

9 Acknowledgments

Laugesen was supported by NSF grant number DMS–9622837. Pugh was partially supported by an NSF post-doctoral fellowship and NSF grant number DMS–9709128. The authors thank Andrea Bertozzi and Kenneth Stolarsky for helpful conversations.

10 Appendices

Appendix A Proof of Theorem 2.1

For $f > 0$, Oron and Rosenau [38] showed $C = 0$ for positive periodic steady states. Under the assumption that $f(0) = 0$ and $|g(0)| < \infty$, Bertozzi and Pugh [13, §2] observed that $C = 0$ if h touches down and at the contact line, h_x vanishes and h_{xxx} is bounded. Using Theorem A.1 below, we prove that $C = 0$ for our larger class of coefficients f and g and larger class of steady-state solutions.

We can assume $C \geq 0$ and $f(h(x_0)) \geq 0$ for some x_0 , as we now explain. If there is no x_0 such that $f(h(x_0)) \geq 0$ then we replace f , g , and C by their negatives. Then if $C < 0$, we replace x with $-x$ to make $C > 0$.

For an equal contact angle touchdown steady state h , applying Theorem A.1 to the support of h (the interval (c, d)) yields $C \not> 0$ and so $C = 0$. For a positive periodic steady state we take a and b to be consecutive global minimum points so that $h(x) > h(a)$ on (a, b) , and again Theorem A.1 implies $C = 0$. This proves Theorem 2.1.

Theorem A.1 *Let $h \in C^1[a, b] \cap C^3(a, b)$ and let f and g be continuous on $(0, \infty)$. Assume*

$$\begin{aligned} h(x) &> h(a) = h(b) \geq 0 \\ f(h(x))h'''(x) + g(h(x))h'(x) &> 0 \end{aligned} \tag{A1}$$

for all $x \in (a, b)$, and that $f(h(x_0)) \geq 0$ for some $x_0 \in (a, b)$.

Then $h'(a) > -h'(b) \geq 0$, and $f \circ h > 0$ on (a, b) .

Moreover, the maximum of h occurs at a point x_{max} with $h' > 0$ on (a, x_{max}) and $h' < 0$ on (x_{max}, b) ; thus for each $x_R \in (x_{max}, b]$, a unique point $x_L \in [a, x_{max})$ exists with $h(x_L) = h(x_R)$. The difference $h'(x_L)^2 - h'(x_R)^2$ strictly increases (from 0) as x_R goes from x_{max} to b . Hence $h'(x_L) > -h'(x_R)$.

To prove Theorem A.1, we first state and prove a lemma that is very similar but has some of the theorem's conclusions as hypotheses:

Lemma A.2 *Let $h \in C^1[a, b] \cap C^3(a, b)$ with $h(a) = h(b) \geq 0$. Assume the maximum of h occurs at a point $x_{max} \in (a, b)$ with $h' > 0$ on (a, x_{max}) and $h' < 0$ on (x_{max}, b) ; thus for each $x_R \in (x_{max}, b]$, a unique point $x_L \in [a, x_{max})$ exists with $h(x_L) = h(x_R)$.*

Let f and g be continuous on $(0, \infty)$, with $f \circ h > 0$ on (a, b) . Assume further that

$$f(h(x))h'''(x) + g(h(x))h'(x) > 0 \quad \text{for all } x \in (a, b). \quad (\text{A } 2)$$

Then $h'(x_L) > -h'(x_R)$, and in particular $h'(a) > -h'(b) \geq 0$. Moreover, the difference $h'(x_L)^2 - h'(x_R)^2$ strictly increases (from 0) as x_R increases from x_{max} to b .

Proof Proof of Lemma A.2.

By assumption, h is invertible on $[a, x_{max}]$ and $[x_{max}, b]$. Let x_L and x_R be the inverse functions: x_L sends $[h_a, h_{max}]$ to $[a, x_{max}]$ and x_R sends $[h_b, h_{max}]$ to $[x_{max}, b]$. Note that $h_a = h_b$. Clearly x_L and x_R are C^3 on (h_a, h_{max}) , and

$$\begin{aligned} \frac{1}{2} \frac{d}{dh} \left(\frac{1}{x'_L(h)^2} - \frac{1}{x'_R(h)^2} \right) &= -\frac{x''_L(h)}{x'_L(h)^3} + \frac{x''_R(h)}{x'_R(h)^3} \\ &= h''(x_L) - h''(x_R) \\ &= -\int_{x_L}^{x_R} h'''(x) dx \\ &< \int_{x_L}^{x_R} \frac{g(h(x))}{f(h(x))} h'(x) dx \quad \text{by (A 2)} \\ &= 0 \end{aligned}$$

since $h(x_L) = h(x_R)$. Hence $(h' \circ x_L)^2 - (h' \circ x_R)^2$ is a strictly decreasing function, and it approaches 0 as h approaches h_{max} . The conclusions of the lemma follow, since $h'(x_L) \geq 0$ and $h'(x_R) \leq 0$. \square

Proof Proof of Theorem A.1

We first prove that $f \circ h > 0$ on (a, b) . It suffices to show $f(h(x)) \neq 0$ for all $x \in (a, b)$, since f and h are continuous and $f(h(x_0)) \geq 0$. Assume not, so that $f(h(x_1)) = 0$ for some $x_1 \in (a, b)$. By inequality (A 1), $g(h(x_1))h'(x_1) > 0$, hence $h'(x_1) \neq 0$. If $h'(x_1) > 0$, let \tilde{x} be the first point in (a, b) to the right of x_1 at which $h(\tilde{x}) = h(x_1)$. If $h'(x_1) < 0$, let \tilde{x} be the first point in (a, b) to the left of x_1 at which $h(\tilde{x}) = h(x_1)$. By inequality (A 1), $g(h(\tilde{x}))h'(\tilde{x}) > 0$, hence $h'(\tilde{x})$ and $h'(x_1)$ have the same sign, which is impossible. Therefore $f \circ h > 0$ on (a, b) .

Let $x_{max} \in (a, b)$ be a global maximum of h . Then $h'(x_{max}) = 0$ and $h''(x_{max}) \leq 0$.

By inequality (A 1), $h'''(x_{max}) > 0$. It follows that $h''(x_{max}) < 0$ since otherwise the positivity of $h'''(x_{max})$ would prevent x_{max} from being a maximum.

We prove $h' < 0$ on (x_{max}, b) . Suppose not, and take $c \in (x_{max}, b)$ to be the first point to the right of x_{max} at which $h'(c) = 0$. Then $h''(c) \geq 0$, and inequality (A 1) implies that $h'''(c) > 0$. It follows that $h''(c) > 0$, since otherwise h' could not be negative to the left of c . Hence c is a strict local minimum of h . Take \bar{b} to be the first point to the right of c at which $h'(\bar{b}) = 0$; such a point exists since $h(c) > h(b)$. Let $\bar{a} \in [x_{max}, c)$ be the unique point at which $h(\bar{a}) = h(\bar{b})$. The hypotheses of Lemma A.2 are satisfied on $[-\bar{b}, -\bar{a}]$ with the functions $\bar{h}(x) = h(\bar{b}) - h(-x)$ and

$$\bar{f}(y) = \begin{cases} f(h(\bar{b}) - y), & 0 < y \leq h(\bar{b}) - h(c), \\ f(h(c)), & y > h(\bar{b}) - h(c), \end{cases} \quad \bar{g}(y) = \begin{cases} g(h(\bar{b}) - y), & 0 < y \leq h(\bar{b}) - h(c), \\ g(h(c)), & y > h(\bar{b}) - h(c). \end{cases}$$

Note that $\bar{h}(x)$ attains its maximum at $x = -c$. Lemma A.2 implies $\bar{h}'(-\bar{b}) > -\bar{h}'(-\bar{a}) \geq 0$, which means $h'(\bar{b}) > -h'(\bar{a}) \geq 0$. But $h'(\bar{b}) = 0$ by construction, giving a contradiction. Hence $h' < 0$ on (x_{max}, b) .

We next prove $h' > 0$ on (a, x_{max}) . Assume not, and let $\tilde{a} \in (a, x_{max})$ be the first point to the left of x_{max} at which $h'(\tilde{a}) = 0$; then $h' > 0$ on (\tilde{a}, x_{max}) . Let $\tilde{b} \in (x_{max}, b)$ be the unique point with $h(\tilde{b}) = h(\tilde{a})$. Applying Lemma A.2 on $[\tilde{a}, \tilde{b}]$ yields $0 = h'(\tilde{a}) > -h'(\tilde{b}) \geq 0$, which is impossible. Therefore $h' > 0$ on (a, x_{max}) .

Theorem A.1 follows from Lemma A.2, since we now know $h' > 0$ on (a, x_{max}) and $h' < 0$ on (x_{max}, b) . \square

Theorem A.1 contains as a special case a lemma Beretta [4, Lemma 2.5] used in studying self-similar solutions for power-law coefficients f and g ; the proofs are related.

Appendix B Positive bounded steady states must be periodic

In this paper the only positive steady states we considered were periodic. The following theorem shows this is not as restrictive as it might appear, because for the class of coefficients we are most interested in, positive bounded steady states are automatically periodic.

Theorem B.1 *Let $h \in C^3(\mathbf{R})$ be positive and bounded, and assume f and g are continuous on $(0, \infty)$, with $f > 0$. Suppose there is a constant C with*

$$f(h(x))h'''(x) + g(h(x))h'(x) = C \quad \forall x \in \mathbf{R}. \quad (\text{B1})$$

Then $C = 0$. Furthermore, if $g \circ h \geq 0$ on \mathbf{R} then h is periodic (possibly constant), and if $g \circ h \leq 0$ on \mathbf{R} then h is constant.

A similar theorem holds when $f < 0$, just by replacing f, g and C with their negatives. Our proof of Theorem B.1 relies on the following lemma:

Lemma B.2 *Let f and g be continuous on $(0, \infty)$, and let $h \in C^3(\mathbf{R})$ be positive with $\liminf_{x \rightarrow \infty} h(x) = 0$ and $\liminf_{x \rightarrow -\infty} h(x) = 0$. Then $f(h(\tilde{x}))h'''(\tilde{x}) + g(h(\tilde{x}))h'(\tilde{x}) = 0$ for some \tilde{x} .*

Proof Proof of Lemma B.2

Fix $x_0 \in \mathbf{R}$. Then we can assume $f(h(x_0)) \geq 0$, perhaps after replacing f and g with their negatives. Now suppose the conclusion of the Lemma fails, so that

$$f(h(x))h'''(x) + g(h(x))h'(x) > 0 \quad \forall x$$

(replace x with $-x$, if necessary).

Let $0 < \varepsilon < h(x_0)$. Write $a(\varepsilon) < x_0$ for the first point a to the left of x_0 at which $h(a) = \varepsilon$, and write $b(\varepsilon) > x_0$ for the first b to the right of x_0 with $h(b) = \varepsilon$: clearly $a(\varepsilon)$ and $b(\varepsilon)$ exist because $\liminf_{x \rightarrow \pm\infty} h(x) = 0$. Then $h > \varepsilon$ between $a(\varepsilon)$ and $b(\varepsilon)$.

Theorem A.1 applies to h on $(a(\varepsilon), b(\varepsilon))$, and hence $h' > 0$ on $(a(\varepsilon), x_{max})$ and $h' < 0$ on $(x_{max}, b(\varepsilon))$. Note that $a(\varepsilon) \downarrow -\infty$ and $b(\varepsilon) \uparrow \infty$ as $\varepsilon \downarrow 0$, because on each *finite* interval, h is bounded away from 0. Hence we deduce that $h' > 0$ on $(-\infty, x_{max})$ and $h' < 0$ on (x_{max}, ∞) . Theorem A.1 further shows that $h'(x_L)^2 - h'(x_R)^2$ increases with x_R , and so

$$\lim_{x_R \rightarrow \infty} [h'(x_L)^2 - h'(x_R)^2] > 0,$$

which implies $\liminf_{x_L \rightarrow -\infty} h'(x_L) > 0$. Thus $h'(x)$ is bounded below by a positive constant for all sufficiently negative x , which is impossible since h is positive. This contradiction completes the proof of the lemma. \square

Proof Proof of Theorem B.1

Assume $C \neq 0$. Then Lemma B.2 implies either $\liminf_{x \rightarrow \infty} h(x) > 0$ or $\liminf_{x \rightarrow -\infty} h(x) > 0$. Assume first that $\liminf_{x \rightarrow \infty} h(x) > 0$. Then $h(x)$ is bounded above and below by positive constants on $[0, \infty)$, and hence so is $1/(f \circ h)$. Also, $F \circ h$ is bounded on $[0, \infty)$, where F is an antiderivative of g/f . By equation (B 1),

$$\begin{aligned} h''(x) &= h''(0) + \int_0^x h'''(s) ds \\ &= h''(0) + C \int_0^x \frac{1}{f(h(s))} ds - F(h(x)) + F(h(0)). \end{aligned}$$

Since $C \neq 0$, this implies that $|h''(x)| \rightarrow \infty$ as $x \rightarrow \infty$, which is impossible since h is positive and bounded. A similar contradiction arises if $\liminf_{x \rightarrow -\infty} h(x) > 0$.

This proves $C = 0$. Dividing (B 1) by $f(h(x))$ and then integrating gives $h''(x) + F(h) - D = 0$ for some constant D , and so the remaining claims in the theorem follow from Lemma B.3 below, applied with $F - D$ in place of F . \square

We now classify solutions of the nonlinear oscillator equation.

Lemma B.3 *Suppose $h \in C^2(\mathbf{R})$ is positive and $h'' + F(h) = 0$ for some $F \in C^1(0, \infty)$. Then h has one of the shapes:*

- (1) **Bump.** h has a strict maximum point x_{max} about which it is symmetric, with $h' > 0$ on $(-\infty, x_{max})$ and $h' < 0$ on (x_{max}, ∞) .
- (2) **Dip.** h has a strict minimum point x_{min} about which it is symmetric, with $h' < 0$ on $(-\infty, x_{min})$ and $h' > 0$ on (x_{min}, ∞) .

- (3) **Periodic.** h is periodic, and as it oscillates, h increases ($h' > 0$) from a strict local minimum to a strict local maximum and then decreases ($h' < 0$) to a strict local minimum, in a symmetric fashion.
- (4) **Monotonic.** $h' > 0$ or $h' \equiv 0$ or $h' < 0$.

Now suppose h is bounded. If $F' \circ h \geq 0$ then h is either constant or Periodic, and if $F' \circ h \leq 0$ then h is constant.

Proof Proof of Lemma B.3

Assume h is nonconstant, so that $h'(\tilde{x}) \neq 0$ for some \tilde{x} . We can suppose $h'(\tilde{x}) > 0$, by considering $h(2\tilde{x} - x)$ if necessary. Let (a, b) be the largest open interval containing \tilde{x} on which $h' > 0$. Suppose first $a = -\infty$. If $b = \infty$ then h is Monotonic; thus we suppose $b < \infty$. Then $h'(b) = 0, h''(b) \leq 0$. Also

$$h'(x)^2 + 2 \int_{h(b)}^{h(x)} F(y) dy = 0 \quad \forall x. \quad (\text{B2})$$

If $h''(b) < 0$ then $h' < 0$ just to the right of b , and from (B2) we deduce $h(x)$ is symmetric about $x = b$: thus h is a Bump. If $h''(b) = 0$ then $F(h(b)) = 0$ and so $h'(x) = O(h(x) - h(b))$, which implies

$$1 = \int_{h(b-1)}^{h(b)} \frac{dx}{dh} dh \geq (\text{const.}) \int_{h(b-1)}^{h(b)} \frac{1}{|h - h(b)|} dh = \infty;$$

this contradiction ensures $h''(b) \neq 0$. This completes the case $a = -\infty$. If $a > -\infty$, similar arguments show h is either a Dip or is Periodic.

We have classified all solutions h into the above four types. Now consider the more restrictive case where either $F' \circ h \geq 0$ or $F' \circ h \leq 0$. Again, we assume h is nonconstant. Then $h''(x_0) > 0$ for some x_0 , since h is a positive nonconstant function and hence is not concave on \mathbf{R} .

Assume $F' \circ h \geq 0$, so that F is increasing on the range of h . Then $h''(x) \geq h''(x_0) > 0$ whenever $h(x) < h(x_0)$, because $h''(x_0) = -F(h(x_0)) > 0$ and F is increasing. It follows that h has a local minimum x_{min} , either at x_0 or to one side of x_0 , with $h''(x_{min}) > 0$. Hence h cannot be Monotonic or a Bump. Similar arguments (using the boundedness of h) show that to the right of x_{min} , h increases to a local maximum, and so h is not a Dip. Hence h must be Periodic.

Next assume $F' \circ h \leq 0$, so that F is decreasing on the range of h . Then $h''(x) > 0$ whenever $h(x) > h(x_0)$, because $h''(x_0) = -F(h(x_0)) > 0$ and F is decreasing. It follows that h is unbounded on one side of x_0 , a contradiction. Therefore h is constant. \square

Appendix C Positive periodic traveling waves do not exist

We now consider positive traveling wave solutions $h(x, t) = H(x - \gamma t)$ of the evolution equation (1.1), with wave speed $\gamma \neq 0$. Boatto, Kadanoff and Olla [14] classified all traveling waves in the special case when $g \equiv 0$ and $f(y) = y^n$. We are interested in $g \neq 0$.

We first assume $f(y) > 0$ for all $y > 0$, and g is continuous. Then the non-existence of

positive periodic traveling waves follows from dissipation of the Lyapunov functional

$$\mathcal{E}(h) = \int_0^P \left\{ \frac{1}{2} h_x^2 - G(h) \right\} dx$$

that was introduced by Bertozzi and Pugh [13, §2] (generalizing [20, 38]), where G is any function with $G'' = g/f$. Indeed, if $h(x, t)$ is a smooth, positive, periodic solution of (1.1) then

$$\frac{d}{dt} \mathcal{E}(h) = - \int_0^P \frac{1}{f(h)} [f(h)h_{xxx} + g(h)h_x]^2 dx.$$

The righthand side is negative unless $f(h)h_{xxx} + g(h)h_x \equiv 0$, which occurs only when h is a steady state of (1.1). Thus if $h(x, t) = H(x - \gamma t)$ is a non-constant positive periodic traveling wave solution then the Lyapunov functional is strictly dissipated. But clearly the Lyapunov functional is constant in time for a traveling wave, and so non-constant positive periodic traveling waves cannot exist. The same reasoning works if $f(y) < 0$ for all $y > 0$.

In fact there are no positive periodic traveling waves even if one removes the constraint that f assumes just one sign. If h is a traveling wave solution of (1.1) then the function H satisfies the ordinary differential equation

$$-\gamma H'(x) = -[f(H(x))H'''(x) + g(H(x))H'(x)]' \quad \forall x \in \mathbf{R}.$$

Without loss of generality, we take $\gamma = 1$; one can ensure this by dividing f and g by γ . The above ordinary differential equation is exact and so for some constant C ,

$$H(x) - C = f(H(x))H'''(x) + g(H(x))H'(x). \quad (\text{C1})$$

We prove there are no nonconstant positive periodic traveling wave solutions:

Theorem C.1 *If f and g are continuous functions on $(0, \infty)$ and $C \in \mathbf{R}$ then there is no nonconstant positive periodic function $H \in C^3(\mathbf{R})$ satisfying (C1).*

Proof

Suppose such an H and C do exist. Let $y \in [H_{min}, H_{max}] \setminus \{C\}$. We first show $f(y) \neq 0$. Assume instead that $f(y) = 0$, so that if $H(x_0) = y$ then (C1) implies $g(y)H'(x_0) = y - C \neq 0$. Therefore H has the same nonzero slope at all such x_0 , which is impossible.

We now show C lies strictly between H_{min} and H_{max} . Assume not. Assume $C \leq H_{min}$. Then $f(y) \neq 0$ for $y \in (H_{min}, H_{max}]$, and so either $f > 0$ or $f < 0$ on $(H_{min}, H_{max}]$. Let P be the period of H and let c be a minimum point, $H(c) = H_{min}$. Define $\mathcal{N} = \{x \in (c, c + P) \mid H(x) > H_{min}\}$. We deduce from (C1) that

$$0 = H''(c + P) - H''(c) = \int_c^{c+P} H'''(x) dx = \int_{\mathcal{N}} \frac{H(x) - C}{f(H(x))} dx \neq 0. \quad (\text{C2})$$

This contradiction implies $C > H_{min}$. Similarly, $C \geq H_{max}$ leads to a contradiction.

Therefore, $H_{min} < C < H_{max}$, and hence $f(H_{max}) \neq 0$. Without loss of generality, we assume $f(H_{max}) > 0$. The continuity of f implies that one of two cases must hold:

- (i) $f(y) > 0$ when $y \in (C, H_{max}]$ and $f(y) > 0$ when $y \in [H_{min}, C)$, or

(ii) $f(y) > 0$ when $y \in (C, H_{max}]$ and $f(y) < 0$ when $y \in [H_{min}, C)$.

Assume that case (i) holds. Choose $c_1, c_2 \in \mathbf{R}$ such that $H(c_1) = C = H(c_2)$ and $H(x) > C$ for all $x \in (c_1, c_2)$. Since $H(x) - C > 0$ and $f(H(x)) > 0$ for all $x \in (c_1, c_2)$, Theorem A.1 implies $H'(c_1) > -H'(c_2) \geq 0$. Next, since H is periodic, $|H'|$ when restricted to the set $\{x \in \mathbf{R} | H(x) = C\}$ does achieve its maximum at some point c_4 , with $H(c_4) = C$. Assume $H'(c_4) < 0$. Choose $c_3 < c_4$ with $H(c_3) = C$ and $H(x) > C$ on (c_3, c_4) . Again one can apply Theorem A.1, deducing that $H'(c_3) > -H'(c_4) = |H'(c_4)|$. This contradicts how c_4 was chosen. Therefore $H'(c_4) > 0$. Now choose $c_3 < c_4$ with $H(c_3) = C$ and $H(x) < C$ on (c_3, c_4) . Applying Theorem A.1 to the function $C - H$ yields $|H'(c_3)| > |H'(c_4)|$, again contradicting the choice of c_4 . Therefore case (i) can never occur.

Now assume case (ii) holds. Choose c with $H(c) = C$ and define $\mathcal{N} = \{x \in (c, c + P) | H(x) \neq C\}$. Repeating the calculations up through (C2) yields a contradiction; in this case the “ $\neq 0$ ” becomes “ > 0 ”. Thus case (ii) can never happen, finishing the proof. \square

Appendix D Proof of (a)–(c) in Theorem 3.1

We first establish a lemma on the invertibility of real analytic functions:

Lemma D.1 *Let $q > 0$ and suppose $\sigma(s)$ is real analytic near $s = 0$, with $\sigma(0) = 1$. Then a function $\tau(t)$ exists that is real analytic near $t = 0$ and satisfies*

$$t = s\sigma(s^q) \quad \iff \quad s = t\tau(t^q) \quad (\text{D1})$$

for all small $s, t > 0$. Also, $\tau(0) = 1$ and $\tau'(0) = -\sigma'(0)$.

Proof Proof of Lemma D.1 By raising the equations in (D1) to the q -th power, then replacing s and t by $s^{1/q}$ and $t^{1/q}$ respectively, we see that τ must satisfy

$$t = s\sigma(s)^q \quad \iff \quad s = t\tau(t)^q \quad (\text{D2})$$

for all small $s, t > 0$. To determine τ , first define $t(s) = s\sigma(s)^q$ and note that $t(s)$ is real analytic and invertible for small s , since $\sigma(0) = 1$, and that $t'(0) = 1$. Writing $s = s(t)$ for the inverse, we have $s(0) = 0$ and $s'(0) = 1$. Since $s(t)/t$ is analytic and equals 1 at $t = 0$, we can define $\tau(t) = (s(t)/t)^{1/q}$. By construction, τ is real analytic and (D2) holds. Also, $\tau(0) = 1$ and $\tau'(0) = -\sigma'(0)$. \square

Proof Proof of (a) in Theorem 3.1: the $q > 0$ case

We take the contact line as occurring at $x = 0$, with the steady state identically zero for small $x < 0$ and positive for small $x > 0$.

Expand $[1 - k^q/(1+q)]^{-1/2}$ in (3.10) as a power series in k^q , then integrate, giving

$$x(k_0) = \sqrt{2q}\sqrt{k_0} \tilde{\sigma}(k_0^q), \quad 0 \leq k_0 < (1+q)^{1/q},$$

where $\tilde{\sigma}$ is a convergent power series. Squaring shows that $x^2/2q = k_0\sigma(k_0^q)$, where $\sigma = \tilde{\sigma}^2$ is real analytic with $\sigma(0) = 1$ and $\sigma'(0) = (1+q)^{-1}(1+2q)^{-1}$. Lemma D.1 then

implies that a real analytic function $\tau(t)$ exists such that

$$k_0(x) = \frac{x^2}{2q} \tau\left(\left(\frac{x^2}{2q}\right)^q\right) = \frac{x^2}{2q} \left(1 - \frac{1}{(2q)^q(1+q)(1+2q)} x^{2q} + O(x^{4q})\right).$$

Since the second coefficient of the power series is nonzero, it determines the regularity of the solution: $k_0 \in C^{1+[2q],\eta}$. \square

Proof Proof of (b) in Theorem 3.1: the $q = 0$ case

In this case, we prove the following asymptotic behaviour for $k_0(x)$ as $x \rightarrow 0$:

$$k_0(x) \sim x^2 \log \frac{1}{x}, \quad k_0'(x) \sim 2x \log \frac{1}{x}, \quad k_0''(x) \sim 2 \log \frac{1}{x}.$$

It follows that $k_0 \in C^{1,\eta}$ for all $\eta \in (0, 1)$. Note that $k_0 \notin C^{1,1}$, since $k_0'(0) = 0$ while $k_0''(x) \rightarrow \infty$ as $x \rightarrow 0$.

To establish the asymptotic formulas, start by changing variable in (3.11) with $v = \sqrt{u^2 - u_0^2}$. This implies

$$x(k_0)u_0 e^{u_0^2} = \sqrt{e} \int_0^\infty 2ve^{-v^2} \frac{u_0}{\sqrt{v^2 + u_0^2}} dv \rightarrow \sqrt{e} \quad (\text{D 3})$$

as $u_0 \rightarrow \infty$ (i.e., as $k_0 \rightarrow 0$ or $x \rightarrow 0$). Therefore

$$k_0(x) = e^{1-2u_0^2} \sim x^2 u_0^2$$

as $x \rightarrow 0$. Also,

$$u_0^2 \sim \log \frac{1}{x},$$

which can be deduced from (D 3) by considering $\log(xu_0 e^{u_0^2})/u_0^2$. Hence $k_0(x) \sim x^2 \log 1/x$. Further,

$$k_0'(x) = \frac{1}{x'(k_0)} = \sqrt{2}\sqrt{k_0}\sqrt{1 - \log k_0} = 2\sqrt{k_0}u_0 \sim 2x \log \frac{1}{x},$$

and

$$k_0''(x) = -\log k_0(x) = -\log[x^2 \log 1/x] + o(1) \sim 2 \log \frac{1}{x}.$$

\square

Proof Proof of (c) in Theorem 3.1: the $-1 < q < 0$ case

Expand $[k^q/(1+q)-1]^{-1/2}$ in (3.12) as $k^{|q|/2}$ times a power series in $k^{|q|}$, then integrate, yielding

$$x(k_0) = \sqrt{2|q|} \frac{\sqrt{1+q}}{1+|q|} k_0^{(1+|q|)/2} \tilde{\sigma}(k_0^{|q|}), \quad 0 \leq k_0 < (1+q)^{1/q},$$

where $\tilde{\sigma}$ is real analytic with $\tilde{\sigma}(0) = 1$. Raising the equation to the power $2/(1+|q|)$,

$$\left(\frac{(1+|q|)^2}{1+q} \frac{x^2}{2|q|}\right)^{\frac{1}{1+|q|}} = k_0 \sigma(k_0^{|q|}),$$

where $\sigma = \tilde{\sigma}^{2/(1+|q|)}$ is real analytic with $\sigma(0) = 1$. Lemma D.1 then implies that a real analytic function $\tau(t)$ exists such that

$$\begin{aligned} k_0(x) &= \left(\frac{(1+|q|)^2}{1+q} \frac{x^2}{2|q|} \right)^{\frac{1}{1+|q|}} \tau \left(\left(\frac{(1+|q|)^2}{1+q} \frac{x^2}{2|q|} \right)^{|q|(1+|q|)^{-1}} \right) \\ &= x^{\frac{2}{1+|q|}} \left(\frac{(1+|q|)^2}{2|q|(1+q)} \right)^{\frac{1}{1+|q|}} \left[1 + O \left(x^{2|q|(1+|q|)^{-1}} \right) \right]. \end{aligned}$$

The regularity is determined by the leading order term: $k_0 \in C^{1,\eta}$ with $\eta = \frac{2}{1+|q|} - 1$. □

We close by noting that if a pair of identical droplets abut, with one droplet supported on $(-P, 0)$ and the other on $(0, P)$, then one can regard the steady state as being even about the contact line $x = 0$. The power series expansion for $k_0(x)$ is then valid for all small values of x , with the modification that x^{2q} is replaced by $|x|^{2q}$. Hence if q is a positive integer then k_0 is infinitely differentiable at the contact line, since $|x|^{2q} = x^{2q}$.

References

- [1] M. Abramowitz and I. A. Stegun. *Handbook of Mathematical Functions*. Dover Publications, New York, 1972.
- [2] G. I. Barenblatt. *Scaling, self-similarity, and intermediate asymptotics*. Cambridge University Press, 1996.
- [3] J. T. Beale and D. G. Schaeffer. Nonlinear behavior of model equations which are linearly ill-posed. *Commun Part Diff Eq*, 13(4):423–467, 1988.
- [4] E. Beretta. Selfsimilar source solutions of a fourth order degenerate parabolic equation. *Nonlinear Anal-Theor*, 29(7):741–760, 1997.
- [5] E. Beretta, M. Bertsch, and R. Dal Passo. Nonnegative solutions of a fourth order nonlinear degenerate parabolic equation. *Arch Ration Mech An*, 129:175–200, 1995.
- [6] F. Bernis. Finite speed of propagation and continuity of the interface for slow viscous flows. *Adv. Differential Equations*, 1(3):337–368, 1996.
- [7] F. Bernis. Finite speed of propagation for thin viscous flows when $2 \leq n < 3$. *CR Acad Sci I-Math*, 322:1169–1174, 1996.
- [8] F. Bernis and A. Friedman. Higher order nonlinear degenerate parabolic equations. *J Differ Equations*, 83:179–206, 1990.
- [9] A. Bertozzi and M. Pugh. Presented at 1997 APS Division of Fluid Dynamics meeting, November 1997.
- [10] A. L. Bertozzi, M. P. Brenner, T. F. Dupont, and L. P. Kadanoff. Singularities and similarities in interface flow. In L. Sirovich, editor, *Trends and Perspectives in Applied Mathematics*, volume 100 of *Applied Mathematical Sciences*, pages 155–208. Springer-Verlag, New York, 1994.
- [11] A. L. Bertozzi and M. Pugh. The lubrication approximation for thin viscous films: the moving contact line with a ‘porous media’ cut off of Van der Waals interactions. *Nonlinearity*, 7:1535–1564, 1994.
- [12] A. L. Bertozzi and M. Pugh. The lubrication approximation for thin viscous films: regularity and long time behavior of weak solutions. *Commun Pur Appl Math*, 49(2):85–123, 1996.
- [13] A. L. Bertozzi and M. C. Pugh. Long-wave instabilities and saturation in thin film equations. *Commun Pur Appl Math*, 51:625–661, 1998.

- [14] S. Boatto, L. Kadanoff, and P. Olla. Traveling wave solutions to thin film equations. *Phys Rev E*, 48:4423–4431, 1993.
- [15] J. P. Burelbach, S. G. Bankoff, and S. H. Davis. Nonlinear stability of evaporating/condensing liquid films. *J Fluid Mech*, 195:463–494, 1988.
- [16] J. P. Burelbach, S. G. Bankoff, and S. H. Davis. Steady thermocapillary flows of thin liquid layers. II. Experiment. *Phys Fluids A–Fluid*, 2:322–333, 1990.
- [17] R. Caffisch and O. Orellana. Long time existence for a slightly perturbed vortex sheet. *Commun Pur Appl Math*, 39(6):807–838, 1986.
- [18] C. Chicone. The monotonicity of the period function for planar Hamiltonian vector fields. *J Differ Equations*, 69:310–321, 1987.
- [19] P. G. de Gennes. Wetting: statics and dynamics. *Rev Mod Phys*, 57(3):827–863, 1985.
- [20] R. J. Deissler and A. Oron. Stable localized patterns in thin liquid films. *Phys Rev Lett*, 68(19):2948–2951, May 1992.
- [21] E. B. Dussan V. The moving contact line: the slip boundary condition. *J Fluid Mech*, 77:665–684, 1976.
- [22] P. Ehrhard. The spreading of hanging drops. *J Colloid Interf Sci*, 168:242–246, 1994.
- [23] P. Ehrhard and S. H. Davis. Non-isothermal spreading of liquid drops on horizontal plates. *J Fluid Mech*, 229:365–388, 1991.
- [24] J. E. Furter and J. C. Eilbeck. Analysis of bifurcations in reaction–diffusion systems with no–flux boundary–conditions – the Selkov model. *P Roy Soc Edinb A*, 125:413–438, 1995.
- [25] R. Goldstein, A. Pesci, and M. Shelley. Instabilities and singularities in Hele–Shaw flow. *Phys Fluids*, 10(11):2701–2723, 1998.
- [26] R. E. Goldstein, A. I. Pesci, and M. J. Shelley. Topology transitions and singularities in viscous flows. *Phys Rev Lett*, 17(20):3043–3046, 1993.
- [27] H. P. Greenspan. On the motion of a small viscous droplet that wets a surface. *J Fluid Mech*, 84:125–143, 1978.
- [28] P. J. Haley and M. J. Miksis. The effect of the contact line on droplet spreading. *J Fluid Mech*, 223:57–81, 1991.
- [29] P. S. Hammond. Nonlinear adjustment of a thin annular film of viscous fluid surrounding a thread of another within a circular cylindrical pipe. *J Fluid Mech*, 137:363–384, 1983.
- [30] J. N. Israelachvili. *Intermolecular and surface forces*. Academic Press, New York, 1992. Second edition.
- [31] O. E. Jensen. The thin liquid lining of a weakly curved cylindrical tube. *J Fluid Mech*, 345:373–403, 1997.
- [32] M. A. Lewis. Spatial coupling of plant and herbivore dynamics — the contribution of herbivore dispersal to transient and persistent “waves” of damage. *Theor Popul Biol*, 45(3):277–312, 1994.
- [33] P. Neogi and C. A. Miller. Spreading kinetics of a drop on a rough solid surface. *J Colloid Interf Sci*, 92:338–349, 1984.
- [34] A. Novick–Cohen. A singular minimization problem for droplet profiles. *Eur J Appl Math*, 4:399–418, 1993.
- [35] A. Novick–Cohen and L. A. Peletier. The steady states of one–dimensional Sivashinsky equations. *Q Appl Math*, 50(4):759–777, 1992.
- [36] A. Novick–Cohen and L. A. Peletier. Steady states of the one–dimensional Cahn–Hilliard equation. *P Roy Soc Edinb A*, 123:1071–1098, 1993.
- [37] A. Oron, S. H. Davis, and S. G. Bankoff. Long–scale evolution of thin liquid films. *Rev Mod Phys*, 69(3):931–980, Dec 1997.
- [38] A. Oron and P. Rosenau. Formation of patterns induced by thermocapillarity and gravity.

J Phys II, 2:131–146, 1992.

- [39] A. Oron and P. Rosenau. On a nonlinear thermocapillary effect in thin liquid layers. *J Fluid Mech*, 273:361–374, Aug 1994.
- [40] F. Otto. Lubrication approximation with prescribed non-zero contact angle: an existence result. *Commun Part Diff Eq*, 23:2077–2164, 1998.
- [41] R. Dal Passo, H. Garcke, and G. Grün. On a fourth order degenerate parabolic equation: Global entropy estimates and qualitative behavior of solutions. *SIAM J Math Anal*, 29(2):321–342, 1998.
- [42] F. Rothe. Remarks on periods of planar Hamiltonian systems. *SIAM J Math Anal*, 24:129–154, 1993.
- [43] R. Schaaf. A class of Hamiltonian systems with increasing periods. *J Reine Angew Math*, 363:96–109, 1985.
- [44] R. Schaaf. *Global Solution Branches of Two Point Boundary Value Problems*. Number 1458 in Lecture Notes in Mathematics. Springer-Verlag, Berlin, 1990.
- [45] M. J. Tan, S. G. Bankoff, and S. H. Davis. Steady thermocapillary flows of thin liquid layers. I. Theory. *Phys Fluids A-Fluid*, 2:313–321, 1990.
- [46] E. O. Tuck and L. W. Schwartz. Thin static drops with a free attachment boundary. *J Fluid Mech*, 223:313–324, 1991.
- [47] S. J. VanHook, M. F. Schatz, J. B. Swift, W. D. McCormick, and H. L. Swinney. Long-wavelength surface-tension-driven Bénard convection: experiment and theory. *J Fluid Mech*, 345:45–78, 1997.
- [48] M. B. Williams and S. H. Davis. Nonlinear theory of film rupture. *J Colloid Interf Sci*, 90(1):220–228, 1982.

EMAIL CONTACT: laugesen@math.uiuc.edu, mpugh@math.upenn.edu